Struct Multidisc Optim (2013) 48:437–472
DOI 10.1007/s00158-013-0912-y

REVIEW ARTICLE

Level-set methods for structural topology optimization: a review

N. P. van Dijk · K. Maute · M. Langelaar · F. van Keulen

Received: 10 October 2012 / Revised: 25 January 2013 / Accepted: 8 February 2013 / Published online: 23 March 2013
© Springer-Verlag Berlin Heidelberg 2013

Abstract This review paper provides an overview of different level-set methods for structural topology optimization. Level-set methods can be categorized with respect to the level-set-function parameterization, the geometry mapping, the physical/mechanical model, the information and the procedure to update the design and the applied regularization. Different approaches for each of these interlinked components are outlined and compared. Based on this categorization, the convergence behavior of the optimization process is discussed, as well as control over the slope and smoothness of the level-set function, hole nucleation and the relation of level-set methods to other topology optimization methods. The importance of numerical consistency for understanding and studying the behavior of proposed methods is highlighted. This review concludes with recommendations for future research.

Keywords Review · Topology optimization · Level-set method · Geometry mapping · Regularization

N. P. van Dijk (✉)
Uppsala University, Lägerhyddsvägen 1, Uppsala, Sweden
e-mail: nicovdijk@gmail.com

K. Maute
University of Colorado, Boulder, CO 80309-0429, USA
e-mail: maute@colorado.edu

M. Langelaar · F. van Keulen
Delft University of Technology, Mekelweg 2,
2628 CD Delft, The Netherlands

M. Langelaar
e-mail: M.Langelaar@tudelft.nl

F. van Keulen
e-mail: A.vanKeulen@tudelft.nl

1 Introduction

1.1 Structural topology optimization

In the past three decades Topology Optimization (TO) has become a powerful and increasingly popular tool for designers and engineers in the early stages of the design process (Bendsøe and Sigmund 2003). The aim of TO is to find the geometry of a design in terms of shape and topology to perform a specific task optimally, ranging from discrete grid-like structures to continuum structures (generalized shape optimization), see for instance the work of Eschenauer and Olhoff (2001) and Rozvany (2001, 2009). In contrast to size and shape optimization, TO does not require a close-to-optimal initial design and is able to generate optimal geometries when intuitive design approaches fail, e.g., due to complex interdependencies between design parameters and the structural response (Bendsøe and Sigmund 2003).

The most common TO approaches are density-based, such as homogenization methods, e.g., Bendsøe and Kikuchi (1988), Suzuki and Kikuchi (1991), Allaire et al. (1997) and Hassani and Hinton (1998), and SIMP methods (Bendsøe 1989; Zhou and Rozvany 1991; Rozvany et al. 1992). In these density-based methods the geometry is described via a material distribution of two or more phases, of which usually one represents "no material" (i.e., the void phase). The material distribution is typically discretized using element-wise constant or nodal shape functions (Sigmund and Petersson 1998; Eschenauer and Olhoff 2001). The other major class of TO approaches uses an implicit description of boundaries to parametrize the geometry: level-set-based TO methods (Sethian 1999, 2001; Osher and Fedkiw 2001, 2003; Wang et al. 2003; Allaire et al. 2004).

Level-set Methods (LSMs) for structural TO define the interfaces between material phases implicitly by iso-contours of a Level-set Function (LSF) (Sethian and Wiegmann 2000; Wang et al. 2003; Allaire et al. 2004). This implicit function allows a crisp description of the boundaries. Depending on the representation of the interface in the (numerical) mechanical model, this can improve the accuracy with which the mechanical response is captured in the vicinity of the boundaries and avoids ambiguities of intermediate material phases when using a density-based approach. In contrast to explicit boundary descriptions (e.g., spline-based), level-set-based TO methods allow for a convenient treatment of topological changes. Additionally, the results of most level-set-based TO methods do not involve mesh-dependent spatial oscillations of the interface geometry (e.g., staircasing) which are often encountered in density-based TO methods.

Many formulations and implementations of LSMs for TO have been proposed in the past decade. However, the fundamental commonalities and differences of the different flavors of LSMs are often not clear. Therefore, this paper provides an overview and classification of the techniques used and aims to clarify their relation and interdependence. Furthermore, we identify several issues that need to be addressed in future research.

1.2 LSMs for structural topology and shape optimization

In structural optimization the two-phase material-void problem is the most simple and most frequently treated case. Given an LSF ϕ, LSMs commonly define the material domain Ω, the void domain $D \setminus \Omega$ and the material interface Γ inside the design domain D as,

$$\begin{cases} \phi(\boldsymbol{X}) > c \;\Leftrightarrow\; \boldsymbol{X} \in \Omega \text{ (material)} \\ \phi(\boldsymbol{X}) = c \;\Leftrightarrow\; \boldsymbol{X} \in \Gamma \text{ (interface)} \\ \phi(\boldsymbol{X}) < c \;\Leftrightarrow\; \boldsymbol{X} \in (D \setminus \Omega) \text{ (void)}, \end{cases} \tag{1}$$

where c is a constant (usually $c = 0$) and $\boldsymbol{X}$ is a point in the design domain (Sethian and Wiegmann 2000; Osher and Santosa 2001; Wang et al. 2003; Allaire et al. 2004).[1] Subsequently, we only consider $c = 0$. Changing the LSF alters the shape and possibly the topology of the material domain Ω. For a two-dimensional design, examples of the LSF ϕ and corresponding material domain Ω before and after a design update are shown in Fig. 1.

Level-set-based TO methods are closely related to shape optimization methods. Many approaches exploit shape-sensitivity analysis and only alter the boundaries of the design (e.g., Wang et al. 2003; Allaire et al. 2004). However, rather than representing the geometry explicitly using e.g., splines, level-set-based methods use an implicit description that allows for easy treatment of topological changes. Thus, holes can merge and new connections can be formed. Other techniques, such as topological derivatives, can be incorporated to nucleate new holes in the interior of the material domain (e.g., Yulin and Xiaoming 2004a; Allaire et al. 2005).

Similar to density-based methods, LSMs also require regularization techniques to obtain a well-posed optimization problem (e.g., the work of Ambrosio and Buttazzo 1993), to remove numerical artifacts (e.g., Van Dijk et al. 2012), to improve the convergence behavior (e.g., Wang et al. 2003) and to avoid convergence to sub-optimal local minima (e.g., Van Dijk et al. 2012). Regularization techniques are also often employed to control the geometrical properties of the resulting designs (e.g., Yamada et al. 2010).

This review focuses on LSMs for structural topology and shape optimization. For brevity, we only provide the most essential references. We focus on methods that use an implicit function to identify two or more material phases within the design domain. This includes approaches that map the geometry to a mechanical model using a density distribution (i.e., the Ersatz approach (Wang et al. 2003; Allaire et al. 2004)), but excludes works that use the density distribution directly as optimization variables (e.g., phase field approaches (Bourdin and Chambolle 2003; Wang and Zhou 2004)). We consider LSMs that update the level-set field via the solution of evolution equations, mathematical programming and other methods.

1.3 Development of level-set methods

The concept of LSMs was developed by Osher and Sethian around 1988 to model moving boundaries. Originally, LSMs were mostly used to model the evolution of interfaces in multi-phase flows (e.g., Osher and Sethian 1988; Sussman et al. 1994; Sethian and Smereka 2003) and in image segmentation (e.g., Malladi et al. 1995a, b; Osher and Paragios 2003). The concept of using a level-set-based description of the geometry for TO was suggested as early as 1998 by Haber and Bendsøe (1998). Several researchers started working on level-set-based TO almost simultaneously (Sethian and Wiegmann 2000; De Ruiter and Van Keulen 2000).

Sethian and Wiegmann (2000) proposed a level-set-based algorithm that coupled the idea of (evolutionary) structural optimization (see, for instance, the work of Xie and Steven 1993 and Huang and Xie 2010) with the LSM (Osher and Sethian 1988; Sethian 1999). The mechanical model was discretized by finite differences covering only the material part of the domain. The LSF was altered in the optimization process to move the boundaries and introduce holes based on an evolutionary stress criterion.

[1] Some LSMs reverse the sign in (1) (e.g., Wang and Wang 2006b).

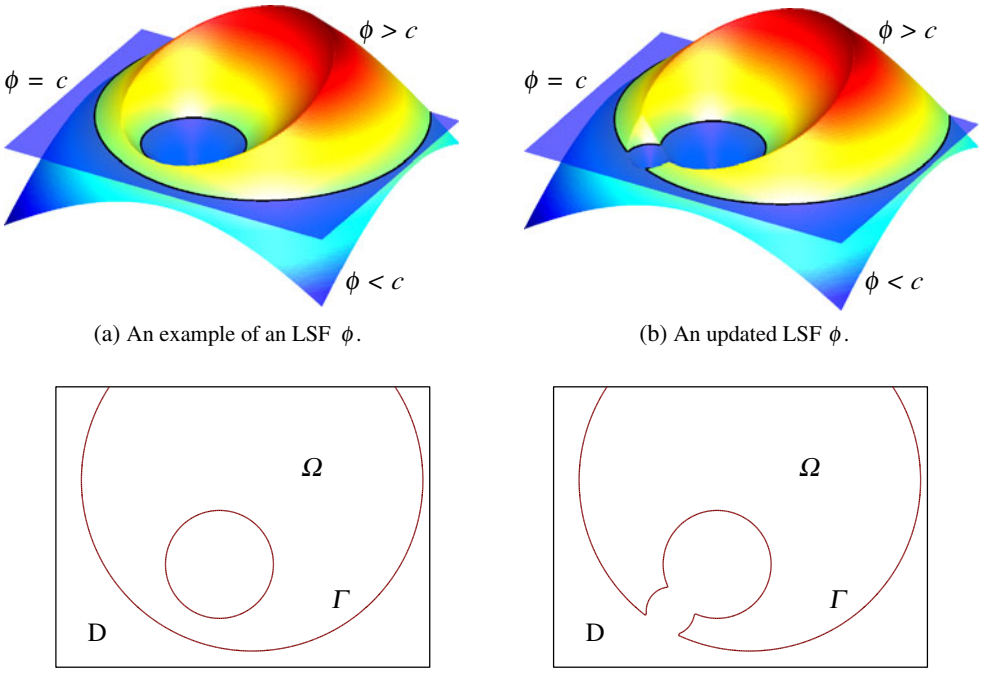

Fig. 1 An example of the LSF ϕ and corresponding material domain Ω before and after a design update

(a) An example of an LSF ϕ.

(b) An updated LSF ϕ.

(c) The material domain Ω corresponding to Fig. 1a.

(d) The updated material domain Ω corresponding to Fig. 1b.

In (2000), De Ruiter and Van Keulen experimented with an approach using Radial Basis Functions (RBFs) and genetic algorithms. Later they investigated an approach that was based on parameter sensitivity information (De Ruiter and Van Keulen 2001) and topological derivatives (De Ruiter and Van Keulen 2002).

Later, Osher and Santosa (2001), Allaire et al. (2002, 2004) and Wang et al. (2003) cast the idea of level-set-based structural optimization into the shape-sensitivity-based optimization framework which remains the most popular approach today.

A mechanism to create new holes inside the structure was first proposed by Eschenauer et al. (1994) and Schumacher (1995). In their research, shape optimization was augmented with a hole-positioning criterion to insert a new hole in the material domain. This idea has been further developed into the mathematical concept of topological derivatives (Sokołowski and Żochowski 1999; Céa et al. 2000; Garreau et al. 2001). Burger et al. (2004), Allaire et al. (2005) and Yulin and Xiaoming (2004a) incorporated topological derivatives in a shape-sensitivity-based level-set formulation.

Initially, the most common approach to advance the LSF was based on the solution of a Hamilton-Jacobi (HJ)-type equation (Osher and Santosa 2001; Wang et al. 2003; Allaire et al. 2004). This approach requires the integration of a pseudo-time-dependent PDE in order to propagate the LSF, similar to the applications of LSMs in multiphase flow simulation and image segmentation. An overview of this type of LSMs has been compiled by Burger and Osher (2005). Gradually, the use of standard mathematical programming algorithms (e.g., MMA (Svanberg 1987)) has become more popular for level-set-based TO increasing the efficiency of the optimization process and constraint handling properties (Wang and Wang 2006b; Luo et al. 2008c; Maute et al. 2011; Otomori et al. 2011; Van Dijk et al. 2012).

1.4 Applications

Starting from two-dimensional compliance minimization and compliant mechanism design optimization, level-set-based topology optimization has been applied to an increasing variety of problems involving different types of design criteria and physics in two and three dimensions.

Level-set-based topology optimization problems have been solved in three dimensions (Allaire et al. 2004; Allaire and Jouve 2005; De Gournay 2006; Zhou and Li 2008; Yamada et al. 2010), involving geometric nonlinearities (Allaire et al. 2004; Kwak and Cho 2005; Luo and Tong 2008; Van Dijk et al. 2010) and shell structures (Park and Youn 2008). Instead of material-void optimization, design optimization of multiple materials can be performed using a level-set approach (Wang and Wang 2004a; Wang et al. 2005; Yulin and Xiaoming 2004b; Luo et al. 2009a; Zhuang et al. 2010).

LSMs have been used to solve eigenvalue (free vibration) problems (Osher and Santosa 2001; Allaire and Jouve 2005; De Gournay 2006; Yamada et al. 2010; Yamasaki et al. 2010a) and contact problems (Myśliński 2008) benefiting from the crisp level-set-based description of the material domain. Problems involving design-dependent loads (e.g., pressure) have also been treated using the LSM (Allaire et al. 2004; Liu and Korvink 2008; Yamada et al. 2011). Because the boundaries can be explicitly tracked in an LSM, in principle design-dependent loads may be taken into account using a crisp description of the interface. However, currently only implementations using a relaxed description of the boundary (i.e., an approximate Dirac delta function, see Section 3) have been demonstrated.

Stress minimization has been tackled using a "black-and-white" implementation of the material domain (Allaire and Jouve 2008) and an X-FEM approach (Van Miegroet and Duysinx 2007). Different methods have been investigated to control the complexity and/or the scale of the geometry (Wang et al. 2007b; Chen et al. 2008; Luo et al. 2008b; Yamada et al. 2010). Also robustness of designs involving uncertainties have been investigated for level-set-based TO methods by De Gournay et al. (2008), Chen et al. (2010) and Chen and Chen (2011).

Furthermore, the LSM has been applied to other types of physical problems, such as problems involving fluids (Amstutz and Andrä 2006; Duan et al. 2008; Zhou and Li 2008; Challis and Guest 2009; Pingen et al. 2010; Kreissl et al. 2011), on thermal (Ha and Cho 2005; Zhuang et al. 2007; Xia and Wang 2008; Iga et al. 2009; Kim et al. 2009; Maute et al. 2011; Yamada et al. 2011), electro-mechanical (Luo et al. 2009a), electro-thermo-mechanical (Luo et al. 2009b), electro-magnetic (Shim et al. 2008; Khalil et al. 2010; Zhou et al. 2010; Lim et al. 2011) and optical problems (Kao et al. 2005; Frei et al. 2007; He et al. 2007). For many of these applications a level-set-based approach can be advantageous because of the crispness of the interface description. However, care has to be taken to retain the crispness of the level-set-based design description in the discretization of the numerical model.

As the above compilation of applications illustrates, LSMs have been successfully applied to a broad range of design problems. However, various issues important for the applicability of LSMs to engineering design problems have not been solved yet, such as effective length-scale control, formulation of manufacturing constraints and ensuring fast and stable convergence behavior. In addition, today's LSMs greatly differ in the formulation of the optimization problems, the parameterization of the LSF, the mapping of the level-set-based geometry onto the structural model, and the strategy for solving the optimization problem. In this paper we will analyze the fundamental similarities and differences as well as the advantages and disadvantages of the different LSMs.

1.5 Structure of LSMs for TO

Level-set-based TO hinges upon three major parts, namely the LSF parameterization, the mechanical model and the optimization strategy, see Fig. 2.

The parameters of the *LSF parameterization* are the optimization variables of a level-set-based TO (e.g., local polynomial shape functions or RBFs). The mechanical model includes the *geometry mapping* and the discretized *structural model*. The geometry mapping projects the geometry described by the discretized LSF onto the structural model that predicts the performance of a candidate design. Both the type of geometry mapping and the structural model influence the predicted behavior of a candidate design. For instance, the geometry mapping can be based on a material distribution (Ersatz material), X-FEM or a conforming mesh. The structural model can involve, for instance, linear elasticity, geometrically nonlinearities or plasticity. A discussion of the various types of structural models is outside the scope of this review.

The desired performance and requirements of a design problem are formulated via the objective and constraints and evaluated using the mechanical model. The strategy to solve this optimization problem includes the choice of *update procedure* (e.g., HJ solvers or mathematical programming) and the type of information used in the update procedure. This information, such as shape-sensitivity analysis, topological

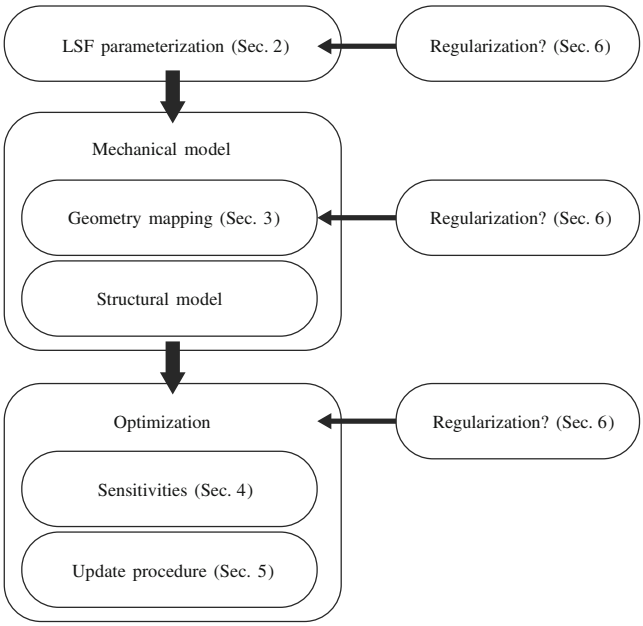

Fig. 2 The components of a level-set-based TO method and corresponding sections

derivatives or discrete derivatives is referred to as the *update information*.

To regularize ill-posedness of the optimization problem, influence the resulting designs and/or improve the convergence behavior of the optimization process, *regularization* are often employed in each of the different components of a level-set-based TO method, such as perimeter penalization or sensitivity smoothening.

1.6 Structure of the paper

A large number of approaches have been used for level-set-based TO. Therefore, this paper starts with a concise overview of the specific options available for each of the components of an LSM: the parameterization of the LSF (Section 2), the geometry mapping (Section 3), the update information (Section 4), the update procedure (Section 5) and regularization (Section 6).

In Section 7, key issues that deserve particular attention are discussed: the convergence rate of an LSM, control over the LSF, hole nucleation and the relation of LSMs to other types of TO methods. Finally, in Section 8 we present our view on the promise and the main challenges of LSMs and provide recommendations for future research.

2 LSF parameterization

The LSF ϕ is discretized in space and parametrized in terms of the optimization variables of the optimization $\boldsymbol{s}$ (e.g., nodal values or coefficients of RBFs). In its most general form this can be written as,

$$\phi = \phi(\boldsymbol{X}, \psi(\boldsymbol{X}, \boldsymbol{s})), \tag{2}$$

where $\boldsymbol{X}$ are the spatial coordinate and ψ is an auxiliary field that may be used for introducing a filtering scheme or other special types of LSF parameterization. The LSF ϕ depends on this auxiliary field ψ, which is controlled by the independent optimization variables $\boldsymbol{s}$.

An example of the definition of a one-dimensional LSF using an auxiliary field ψ is illustrated in Fig. 3. The auxiliary field can be parametrized using, for instance, RBFs $\psi = \sum_i N_i^{\mathrm{RBF}} s_i$. On the other hand, the one-dimensional LSF can be discretized using linear basis functions on a structured grid $\phi = \sum_i N_i^{\mathrm{LIN}} \phi_i$. The nodal values of the LSF now depend on the auxiliary field as $\phi_i = \psi_i(\boldsymbol{X}_i)$. In this manner the LSF ϕ is discretized on a structured grid but controlled using the optimization variables s_i and RBFs (e.g., Kreissl et al. 2011; Van Dijk et al. 2012). The application of any type of filtering scheme on the LSF can also be regarded as using an auxiliary field.

In the simplest case, this auxiliary field is not necessary, i.e. $\phi = \phi(\boldsymbol{X}, \boldsymbol{s})$, and the nodal values of the discretized

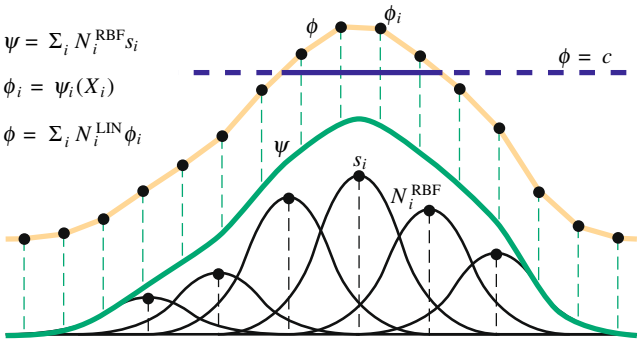

Fig. 3 An example of a one-dimensional LSF ϕ discretized with linear shape functions of which the nodal values ϕ_i depend on an auxiliary field ψ. The auxiliary field ψ is discretized with RBFs and controlled by the optimization variables s_i

LSF can be directly treated as the optimization variables. In the following we consider parameterization methods of the auxiliary field ψ.

The choice of parameterization determines the kind of shapes (design freedom) and the level of detailedness (smallest features) of the zero-level contours of the LSF and may restrict the design space to prevent numerical artifacts caused by the spatial resolution of the discretized structural model. The choice of parameterization of the LSF directly influences the nature of the optimization problem, i.e., the nonlinearity and/or monotonicity of the responses and the dimensionality of the optimization problem, and therefore the effort needed to solve the optimization problem.

On the other hand, the accuracy of the predicted responses is directly related to the spatial resolution of the discretized structural model. Therefore, it is beneficial to decouple the parameterization of the LSF from the discretization of the structural model (Norato et al. 2004; Pingen et al. 2010). By decoupling the design and physical resolution, the discretization of the structural model can be refined to meet a required accuracy while keeping the optimization process efficient. In practice they are often coinciding for implementational convenience, which may lead to numerical artifacts as a result of the interplay between the discretization of the design and the structural model.

The magnitude of the spatial gradient ("steepness") of the LSF along the material boundary determines the sensitivity of the shape of a design to changes of the LSF and, therefore, has an effect on the convergence rate of an LSM (see Section 7.1). The steepness of the LSF is also important for the size of the diffuse interface using density-based geometry mapping (see Section 3.3). Therefore, some control over the slope of the LSF in the vicinity of its zero-level contour is often desired (Wang et al. 2003; Allaire et al. 2004). For instance, many authors (e.g., Wang et al. 2003; Allaire et al. 2004) employ reinitialization algorithms (i.e.,

regularization, see Section 6.1) to maintain the LSF as a signed-distance function, i.e., $\|\nabla\phi\| = 1$.

We can distinguish between the following aspects of the LSF parameterization: the support size of the basis functions, the type of interpolation and the shape of basis functions. It is also possible to describe the LSF as a combination of parametrized LSFs describing basic geometric shapes. These aspects and their implications are discussed in the next subsections.

2.1 Support size of basis functions

The support size of a basis function is the size of the region where the function is non-zero. We distinguish three types of support sizes: local, mid-range and global.

Local basis functions Local basis functions are non-zero in a (small) finite part of the design domain with minimal overlap. In TO, the same interpolation is often used as the finite-element discretization of the mechanical model. A nodal value of the LSF one influences the interpolation in the adjacent elements, see Fig. 4a.

This type of interpolation is used by many authors such as Belytschko et al. (2003), Allaire et al. (2004) and Amstutz and Andrä (2006). In the absence of smoothing regularization, changing a nodal value cannot displace the material interface by more than the size of a single finite element. Therefore, a large number of iterations may be required to move the boundary substantially.

Mid-range basis functions Basis functions of the mid-range type are still only non-zero in a finite part of the design domain (compact). However, the basis functions overlap and in each location in the design domain more basis functions are non-zero, see Fig. 4b.

For instance, Luo et al. (2008c) investigated this type of interpolation with varying amount of overlap. This results in more basis functions having an influence on moving the boundary of the material domain. Compactly supported RBFs are an example of this type of interpolation. Because more optimization variables have an influence on the material boundary, a faster rate of design change may be achieved.

Global functions Global basis functions are non-zero (almost) everywhere in the domain and, therefore, all basis functions overlap, see Fig. 4c.

De Ruiter and Van Keulen (2004), Gomes and Suleman (2006), Wang and Wang (2006b) and Pingen et al. (2010) have employed this kind of basis functions. In this case *all* optimization variables have an influence on the *whole* material boundary. This type of interpolation may lead to a fast rate of design change, but requires additional memory and computational effort due to the interaction of basis functions (Wang et al. 2007c). Furthermore, it can be more difficult to find appropriate step sizes for updating the optimization variables as the cumulative effect of all optimization variables may lead to large changes of the material domain.

Depending on the type of interpolation and the support size, the choice of basis functions strongly influences the maximum level of detail of the material interface that can be represented. For instance, two large and relatively flat Gaussian basis functions cannot describe a small spatial variations of the interface. However, they cannot entirely prevent a small feature of the zero-level *contour* of the LSF (i.e., the design), see Fig. 5.

The number of optimization variables that exert an influence on the movement of a specific part of the boundary depends on the support size and spacing of the associated basis functions. Only optimization variables that have an influence on the boundary have non-zero (consistent) sensitivity information. In a sensitivity-based optimization process, larger support sizes may, therefore, lead to faster movement of the boundary and faster design evolution in the optimization process. Filtering (i.e., smoothing) of the LSF is another option to extend the influence of individual optimization variables.

2.2 Optimization variables

The parameters of the LSF parameterization are defined as a function of the optimization variables. The functional form of this relationship has an influence on the possible variations of the geometry and can even give some control over the magnitude of the gradient of the LSF on the structural boundary, which is important for the numerical stability of the optimization. When an auxiliary field is used in the LSF

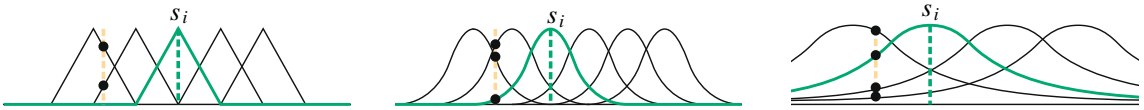

(a) Local basis functions. (b) Mid-range basis functions. (c) Global basis functions.

Fig. 4 Examples of different support sizes of basis functions. The *black dots* indicate how many basis functions are non-zero at an arbitrary location

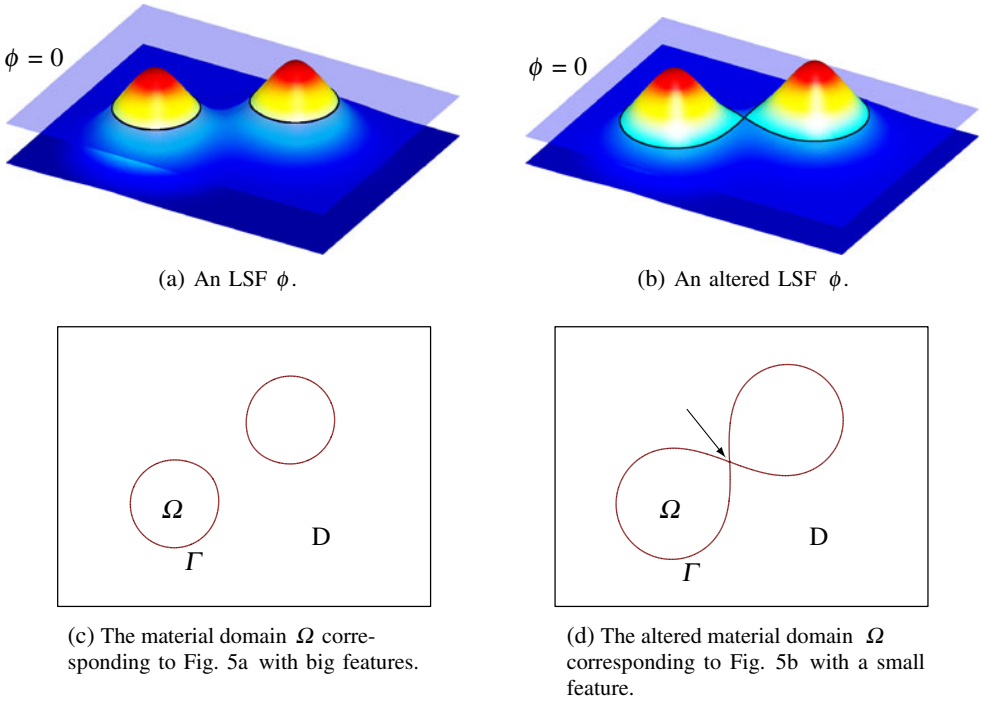

Fig. 5 An LSF ϕ of just two Gaussian basis functions with a large support size and the corresponding material domain Ω

(a) An LSF ϕ.

(b) An altered LSF ϕ.

(c) The material domain Ω corresponding to Fig. 5a with big features.

(d) The altered material domain Ω corresponding to Fig. 5b with a small feature.

parameterization, this discussion should be applied to the auxiliary field ψ.

The LSF is usually defined as the sum of the basis functions ϕ_i as,

$$\phi(\boldsymbol{X}, \boldsymbol{s}) = \sum_{i}^{n} \phi_i(\boldsymbol{X}, s_i). \tag{3}$$

The most frequently adopted functional relations between the basis functions ϕ_i and the optimization variables $\boldsymbol{s}$ are outlined in the following.

Scaling basis functions The most common way to parametrize the LSF is to use a nodal value to scale the basis function as,

$$\phi_i(\boldsymbol{X}, s_i) = s_i N_i(\boldsymbol{X}). \tag{4}$$

This approach, visualized in Fig. 6a, is employed in the majority of LSMs. Without upper and lower bounds, this type of interpolation does not give any control over the gradient of the LSF.

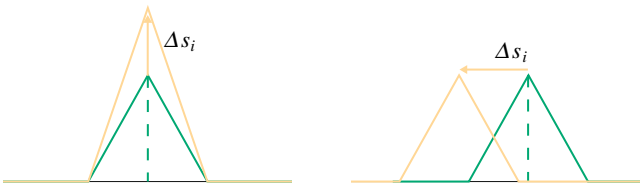

(a) Scaling basis functions.

(b) Translating basis functions.

Fig. 6 Examples of different types of interpolation

Translating basis functions Xing et al. (2007) proposed to use the location of the basis function as the optimization variables, see Fig. 6b. A basis function can be moved through the design domain as,

$$\phi_i(\boldsymbol{X}, \boldsymbol{X}_i) = N_i(\boldsymbol{X} - \boldsymbol{s}_i), \tag{5}$$

where for each basis function and spatial dimension one optimization variable s_i is needed. This approach is also adopted by Ho et al. (2011, 2012), investigating a combination with the partition of unity method to reduce computational costs.

Translating basis functions gives a measure of control over the length scale of the resulting designs and gradient of the LSF. However, the spatial distribution of the basis functions changes during the design optimization, which can lead to a low design resolution in underpopulated parts of the design domain. Also, swapping two basis functions has no effect on the shape of the design resulting in a loss of uniqueness of the optimization problem and convergence issues.

2.3 Type of basis functions

The shape of the basis functions $\phi_i(\boldsymbol{X}, s_i)$ has an influence on the smoothness of the LSF and therefore the material domain.

FEM basis functions The most common choice of parameterizing the LSF is based on finite-element basis functions

(compact) on a fixed mesh (Belytschko et al. 2003; Wang et al. 2003; Allaire et al. 2004; Amstutz and Andrä 2006; Van Dijk et al. 2012). On two-dimensional domains bilinear interpolation on rectangular finite elements is often used for interpolating both the displacements and the LSF, see Fig. 7a (Wang et al. 2003). Other interpolation schemes include (piecewise) linear interpolations on rectangular (Van Dijk et al. 2012) or triangular elements (Liu et al. 2005; Xing et al. 2010). The extension of these kinds of basis functions to three dimensions is straightforward.

Depending on the type of FEM basis function, the gradient of the LSF can change discontinuously between finite elements, e.g., if the LSF is C^0 continuous. In this case, the zero-level contour of the LSF has a non-smooth boundary (sharp corners), which may be disadvantageous for certain applications.

The use of structured and, in particular, uniform meshes provides computational advantages and allows for simplified numerical schemes, for example approximations of the curvature of the LSF using finite-differencing stencils (Wang et al. 2003). Furthermore, structures meshes lead to efficient computational schemes when combining finite difference and upwinding methods; such scheme are frequently used to update the LSF (see Section 5.1) or reinitialize the LSF (see Section 6.1).

Radial Basis Functions (RBFs) RBFs employed to describe the LSF (see Fig. 7b) e.g., by De Ruiter and Van Keulen (2004), Wang and Wang (2006b), Wei and Wang (2006), Luo et al. (2007) and Kreissl et al. (2011). Multi-quadratic splines were used e.g., by Wang and Wang (2006b) and Kreissl et al. (2011). Luo et al. (2007) employed compactly supported polynomial RBFs with varying support radii. De Ruiter and Van Keulen (2004) implemented global Gaussian RBFs in their work. Alternatively, inverse multiquadratic splines were adopted in the work of Xing et al. (2007).

Smoothness of the RBFs ensures that the LSF is inherently smooth, and, therefore, contours of the LSF are generally smooth as well (except in some limit cases, see e.g., Fig. 5). Using RBFs implies overlapping basis functions (RBFs often have a global support size) and a continuous spatial gradient of the LSF over the design domain (as opposed to FEM basis functions). An LSF parameterization based on RBFs is usually decoupled from the discretization of the structural model.

Spectral parameterization Gomes and Suleman (2006) use a spectral parameterization of the LSF, i.e., a Fourier series. The coefficients of the Fourier series are the optimization variables in the level-set-based TO (see Fig. 7c).

A spectral LSF parameterization may be particularly advantageous for optimization of periodic structures. At a sufficiently coarse design resolution, small details cannot be described by this type of parameterization. The non-local nature of the spectral parameterization has the potential advantage of fast design evolution. However, the non-locality may also pose problems as the limited design resolution can result in artifacts such as undulation of structural boundaries (Gomes and Suleman 2006).

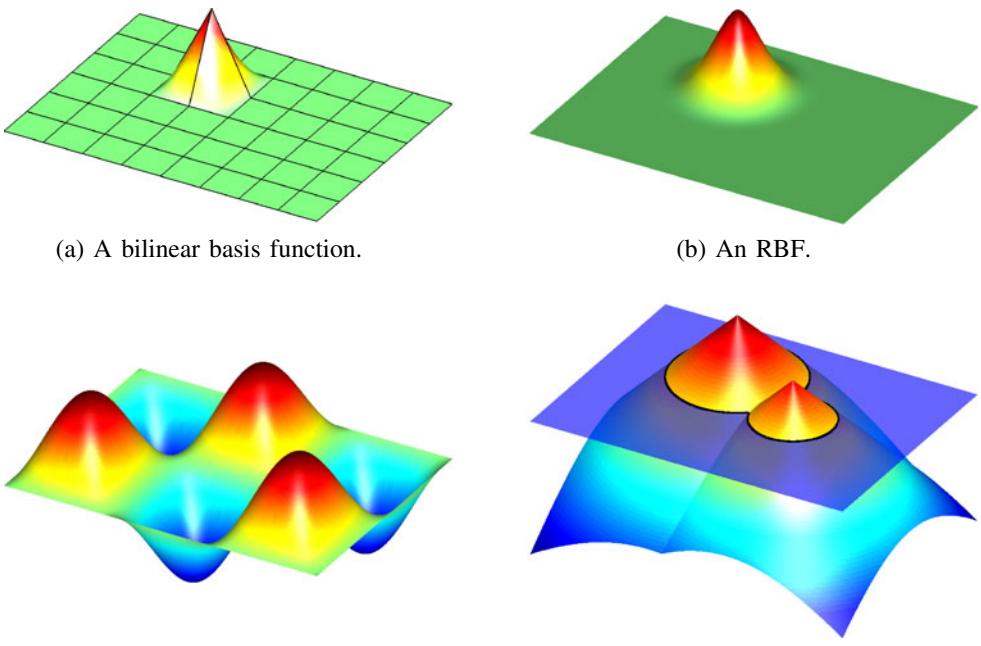

(a) A bilinear basis function. (b) An RBF.

(c) A spectral basis function. (d) Two combined geometric shapes.

Fig. 7 Different types of basis functions in two dimensions

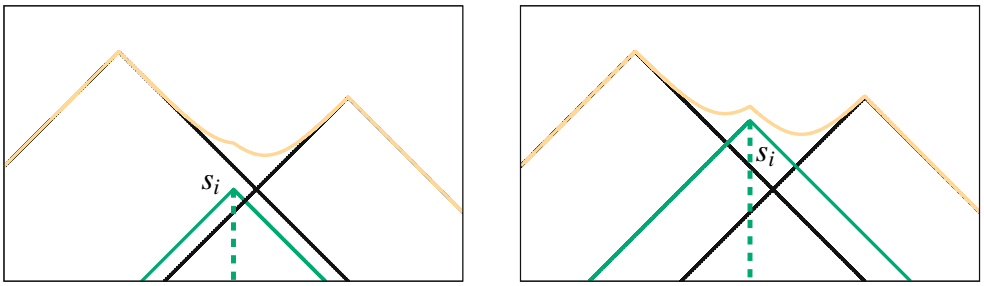

(a) An approximate maximum function.

(b) An altered approximate maximum function.

Fig. 8 Example of an approximate maximum formulation

2.4 Parametrized geometric shapes

A different way to parametrize the LSF is to use a combination of parametrized geometric shapes (Van Miegroet and Duysinx 2007) (e.g., radius of a circular hole, see Fig. 7d). For each geometric shape an LSF is constructed (e.g., signed-distance function) to serve as (global) basis functions ϕ_i. The LSF can now be defined using max and/or min operators performing Boolean operations of the individual shapes described by the separate basis functions ϕ_i, for instance,

$$\phi(\boldsymbol{X}, \boldsymbol{s}) = \max_i \phi_i(\boldsymbol{X}, s_i). \tag{6}$$

Van Miegroet and Duysinx (2007) used this approach involving circles and ellipses to minimize stresses in designs using a level-set approach. The same approach can also be adopted using the basis functions described in the previous subsection (the signed-distance function to a circular hole is in fact a cone-type RBF).

This approach allows constructing a parameterization such that results are manufacturable and only few optimization variables are needed. However, by employing relatively few optimization variables the design freedom is reduced and potentially good designs may be eliminated from the design space. A further drawback of this maximum formulation is that it is not differentiable with respect to the optimization variables $\boldsymbol{s}$.

To overcome this drawback, Pingen et al. (2010) and Kreissl et al. (2011) employ an approximate maximum formulation. For instance, using the p-norm approximation of the maximum (6) becomes,

$$\phi(\boldsymbol{X}, \boldsymbol{s}) = \left[\sum_i^n (\phi_i(\boldsymbol{X}, s_i) + c)^p\right]^{1/p} - c, \tag{7}$$

where the constant c is added to avoid negative contributions of the summand (Pingen et al. 2010). Alternatively, the Kreisselmeier–Steinhauser (KS) function can be used to approximate the maximum operator (Kreisselmeier and Steinhauser 1979; Kreissl et al. 2011). An advantage of this approach is that the gradient of the LSF at the boundary of the material domain can be controlled, see Fig. 8.

2.5 Bounds and initialization

Additionally, upper and lower bounds for the optimization variables may be set. This limits the design space and can provide upper limits for the magnitude of the gradient of the LSF. However, such additional bounds need to be accounted for in the optimization strategy (Kreissl et al. 2011).

When a nonlinear relation is chosen between the LSF and the optimization variables, it is not trivial to find initial optimization variables that lead to an appropriate initial material domain. Using nonlinear least-squares fitting, close approximations to a desired initial configuration can be found.

3 Geometry mapping

An important part of the formulation of a level-set-based TO is the mapping of the geometry to a mechanical model. In this section we discuss the options for the geometry mapping which influences the accuracy of the structural response, in particular near the interface, and the final result of the optimization process. It is emphasized that numerical artifacts can be the result of the geometry mapping. A popular approach is to translate the LSF into a density distribution similar to density-based optimization methods (e.g., Wang et al. 2003; Allaire et al. 2004). Alternatively, the geometry mapping can be based on a discrete description of the material and void domain not involving any intermediate states (e.g., Belytschko et al. 2003; Eschenauer et al. 1994).

In general, the level-set-based geometry description, (1), is used to formulate volume integrals of some functional f (e.g., the weak form of the governing equations) over the material domain in terms of the Heaviside function $H(\phi)$ as,

$$\int_\Omega f dV = \int_D f H(\phi) dV, \tag{8}$$

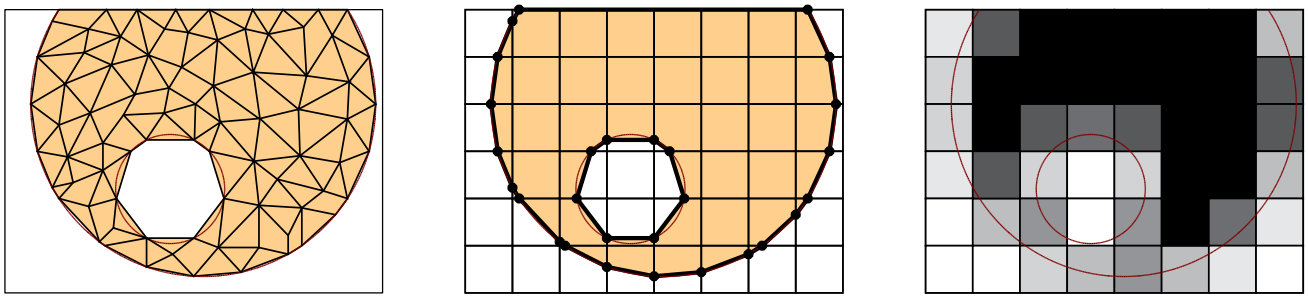

(a) Conforming: Only the material domain is discretized.

(b) Immersed Boundary Technique: Boundary conditions are enforced locally at the interface.

(c) Density-based: In each finite element an element density indicates the amount of material.

Fig. 9 Examples of different types of geometry mapping corresponding to the topology depicted in Fig. 1c

where the Heaviside function $H(\phi)$ is defined as,

$$H(\phi) = \begin{cases} 0 \text{ for } \phi < 0 \\ 1 \text{ for } \phi \geq 0. \end{cases} \tag{9}$$

Similarly, integrals over the material boundary can be formulated in terms of the Dirac delta function $\delta(\phi)$ as,

$$\int_\Gamma g dS = \int_D g\delta(\phi)\|\nabla\phi\| dV. \tag{10}$$

where $\delta(\phi)$ is the one-dimensional Dirac delta function defined by,

$$\delta(\phi) = \begin{cases} +\infty \text{ for } \phi = 0 \\ 0 \quad\ \text{for } \phi \neq 0, \end{cases} \tag{11}$$

and,

$$\int_{-\infty}^{\infty} \delta(\phi) d\phi = 1. \tag{12}$$

There are three different approaches that can be used to implement (8) and (10), see Fig. 9. The discretization can be aligned with the material domain using a conforming discretization or Immersed Boundary Techniques (IBTs). Alternatively, density-based methods can be used to approximate (8) and (10) usually on a fixed regular mesh.

3.1 Conforming discretization

Conforming discretization (Fig. 9a) differs from shape optimization methods (e.g., Eschenauer et al. 1994, Schleupen et al. 2000, Bletzinger et al. 1991; Le et al. 2011) in that shape changes are governed by the evolution of an LSF. This type of discretization provides an accurate model of the performance of a candidate design, in particular along the boundaries. The crisp boundary description is particularly useful for problems require a sharp interface treatment and/or have convergence problems for intermediate states when density-based methods are used. A conforming discretization typically leads to the most accurate prediction of the local structural response along the boundary which is essential for e.g., stress constraints.

Ha and Cho (2008a, b) solved nonlinear structural analyses on unstructured conforming meshes and translated the sensitivity information to a fixed structured level-set grid. Abe et al. (2007) also discretize the LSF on a fixed structured mesh, but employed boundary elements to discretize the structural design in their work. Yamasaki et al. (2011) used a mesh deformation approach to obtain a conforming mesh for the numerical analysis in each step of the optimization process. Also Allaire et al. (2011) proposed to use a type of mesh evolution that results in a conforming discretization.

Conforming discretizations generally provide a good representation of the boundaries in a structural model. However, noise is introduced in the optimization process due to the changing discretization, similar as in classical shape optimization methods (Schleupen et al. 2000). Furthermore, the mesh generation step in each iteration of the optimization process leads to an additional computational burden and potential problems related to meshing arbitrary three-dimensional geometries. Some of the added costs may be compensated by the savings in computation time due to efficient discretization of only the material domain, especially in the case of slim or sparse designs. However, in this case subregions may disconnect from the rest of the material domain leading to an irreversible step in the optimization process and resulting in singular structural analyses.

3.2 Immersed Boundary Techniques

Several Immersed Boundary Techniques (IBTs) have been proposed to obtain an accurate representation of the physical response along the interface while avoiding remeshing. The discretization of the design domain remains fixed,

but the location of the structural boundary is captured in the structural model, see Fig. 9b. This provides a crisp "black-and-white" description of the structural model.

The eXtended Finite Element Method (X-FEM) describes the behavior of the structural boundary using local enrichments of elements cut by the zero-level contour of the LSF (Fries and Belytschko 2010). Boundary conditions are enforced locally at the material interface using different types of immersed boundary techniques (Fries and Belytschko 2010). Volume integrals such as (8) can be evaluated using sub-domains that are locally aligned with the zero-level contour of the LSF. This is in particular useful for problems that involve structural models and do not allow a diffuse treatment of the structural boundary, i.e., where a diffuse interface would result in convergence problems of the mechanical model.

Belytschko et al. (2003) use an X-FEM approach to approximate displacement fields modeling the void phase as a compliant material. For the sensitivity information of the response functions they resort to an approximate Dirac delta function (see Section 4). X-FEM has been used by Maute et al. (2011) for phonon transport problems of heterogeneous materials, allowing the modeling of phonon scattering at the material interfaces. Kreissl and Maute (2012) use an LSM and X-FEM to optimize flow problems described by the incompressible Navier–Stokes equations. The no-slip condition at the fluid-solid interface is enforced via a stabilized Lagrange multiplier formulation.

In the work of Van Miegroet and Duysinx (2007) the displacement fields are calculated using X-FEM for predicting the stresses at the boundary. Instead of the full enrichment of the finite elements, they perform the integration for the element stiffness only over the material part of the finite element. Indeed, when the void is not modeled as a compliant material (i.e., eliminated from the structural analysis) and no external forces act on the emerging boundaries, X-FEM reduces to only performing the stiffness integration over the material part of a finite element (Van Miegroet et al. 2005; Van Miegroet and Duysinx 2007). Wei et al. (2010) report that, even when the void *is* included as a compliant material, the results of X-FEM with and without enrichment are almost equivalent for purely structural solid-void problems. This is not the case for multi-phase problems with comparable stiffnesses of the two phases (Maute et al. 2011).

Boundary conditions can also be enforced locally on the interface using finite difference methods (Sethian and Wiegmann 2000; Kreissl et al. 2011). Sethian and Wiegmann (2000) use jump conditions to account for the discontinuity in the displacement field in a finite difference approximation of the structural equilibrium. Kreissl et al. (2011) locally enforce boundary conditions of the Lattice Boltzmann Method by extrapolating the fluid state in the fluid domain onto the boundary defined by the zero-level contour of the LSF.

A geometry mapping using IBTs allows the enforcement of boundary conditions directly along the interface and does not rely on material interpolation schemes. Therefore, the interface in the structural model is not blurred but strictly "black-and-white". Since the different domains are unambiguously mapped to the analysis model, artificial local minima of the optimization problem caused by material interpolation schemes may be avoided.

Moreover, noise can be introduced in the structural response due to the discretization of the IBT. Van Miegroet and Duysinx (2007) report noise and an ill-conditioning of the discretization of the mechanical model in case of small intersections of finite elements. This can lead to overestimation of stresses when the material fraction of an element relative to its size becomes small.

Furthermore, the optimization process can lead to non-smooth boundaries exploiting particular bad discretization of IBTs causing ill-conditioning of the structural model. In order to avoid this problem Kreissl et al. (2011) employ a filtering approach for smoothing the LSF.

To employ an IBT for the numerical model of a design optimization problem, specialized code is needed. The implementation of IBTs can be difficult and time consuming.

3.3 Density-based mapping

The most common type of geometry mapping is a Eulerian approach referred to as density-based. During the optimization process, the discretization of the design domain of the structural model is kept fixed and the material domain can 'flow' through the mesh (due to design updates). The geometry is described by an intermediate density field $\rho(\boldsymbol{X})$, indicating the amount of material at each point of the design domain (Bendsøe and Sigmund 2003).

The density distribution $0 < \varepsilon \leq \rho(\boldsymbol{X}) \leq 1$ is used to represent solid material ($\rho = 1$) or void ($\rho = \varepsilon$), where ε is a lower bound to avoid singular structural problems, similar to pure density-based TO methods (Bendsøe 1989; Zhou and Rozvany 1991; Eschenauer and Olhoff 2001; Rozvany 2009). The general idea is to replace the Heaviside function in (8) with a density distribution $\rho(\phi)$ and to approximate (8) as,

$$\int_{\mathrm{D}} f H(\phi) dV \approx \int_{\mathrm{D}} f \rho(\phi) dV. \tag{13}$$

The density field is a function of the LSF: $\rho = \rho(\phi)$. A crisp ("black-and-white") representation of the geometry is obtained when an exact Heaviside $H(\phi)$ is used. For instance, a *point-wise* density distribution can be defined as,

$$\rho(\phi) = \varepsilon + (1 - \varepsilon) H(\phi). \tag{14}$$

The exact Heaviside function $H(\phi)$ in (14) cannot be directly differentiated and is, therefore, often replaced with a smooth approximation of the Heaviside function $\tilde{H}(\phi)$, such as a piecewise polynomial,

$$\tilde{H}(\phi) = \begin{cases} 0 & \text{for } \phi < -h \\ -\frac{1}{4}\left(\frac{\phi}{h}\right)^3 + \frac{3}{4}\left(\frac{\phi}{h}\right) + \frac{1}{2} & \text{for } -h \leq \phi \leq h \\ 1 & \text{for } \phi > h, \end{cases} \tag{15}$$

where h is the bandwidth. This results in a smeared representation of the geometry, involving intermediate densities $\varepsilon < \rho < 1$ near the boundary of the material domain.

Alternatively, approximate Heaviside functions based on polynomials (Wang et al. 2003; Liu et al. 2005; Van Dijk et al. 2010; Kawamoto et al. 2011) or trigonometric functions (Belytschko et al. 2003; Haber 2004; Luo et al. 2008a; Pingen et al. 2010) have been used. Examples of the exact and an approximate Heaviside function corresponding to the same LSF are depicted in Fig. 10b and a, respectively.

Similarly, boundary integrals can be approximated using a corresponding approximate Dirac delta function $\tilde{\delta}(\phi) \equiv \partial\tilde{H}/\partial\phi$ in (10) (Osher and Santosa 2001; Belytschko et al. 2003; Guo et al. 2005; Ha and Cho 2005; Luo et al. 2007, 2009b).

Most density-based LSMs use either element-wise constant material fractions or a direct point-wise mapping of the LSF into a density distribution.

Material-fraction approach Element-wise constant material fractions (element densities) $0 < \varepsilon \leq \rho_e \leq 1$ can be used to describe the density distribution, see Fig. 9c. This simplifies (13) to,

$$\int_\Omega f dV \approx \sum_e \rho_e \int_{\mathrm{D}_e} f dV, \tag{16}$$

where D_e is the area/volume of a single element. Often density-based LSMs involve a structured regular grid of finite elements (Wang et al. 2003; Allaire et al. 2004), but other types of finite element discretization are also possible, e.g., De Ruiter and Van Keulen (2004), Liu et al. (2005) and Liu and Korvink (2008).

The element densities are typically defined as the average value of the Heaviside function in each finite element (Allaire et al. 2004; De Ruiter and Van Keulen 2004),

$$\rho_e = \varepsilon + (1-\varepsilon)\frac{\int_{\mathrm{D}_e} H(\phi) dV}{\int_{\mathrm{D}_e} dV}, \tag{17}$$

where the quotient in (17) is exactly the material fraction. In Fig. 10c an example of an element-wise constant density distribution is shown using an exact Heaviside formulation.

With few exceptions (e.g., Van Dijk et al. 2010), usually the exact Heaviside function $H(\phi)$ is used in (17) to obtain the material fraction inside a finite element (Allaire et al. 2004; De Ruiter and Van Keulen 2004; Van Dijk et al. 2012). Intermediate element densities $\varepsilon < \rho_e < 1$ are present, but *only* for elements which are cut by the zero-

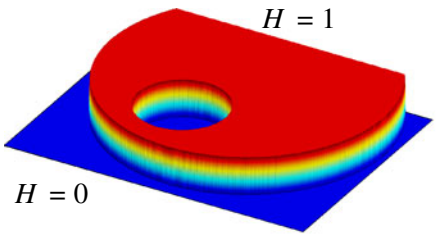

(a) The exact Heaviside function $H(\phi)$ corresponding to Fig. 1a.

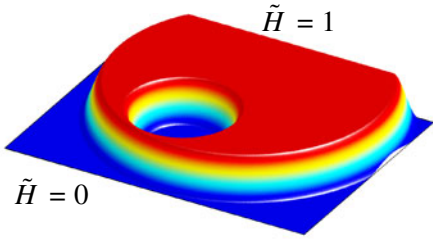

(b) An approximate Heaviside function $\tilde{H}(\phi)$ corresponding to Fig. 1a.

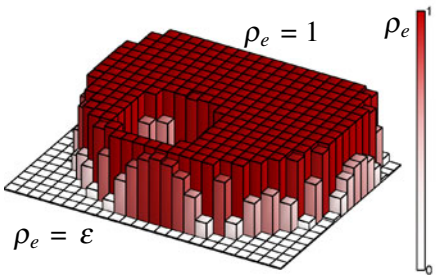

(c) Element densities ρ_e corresponding to the exact Heaviside function $H(\phi)$ of Fig. 10a.

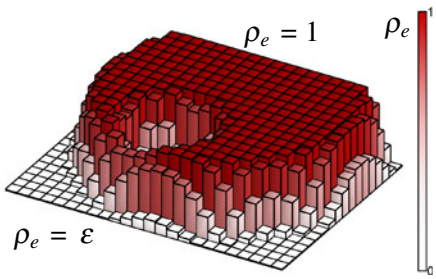

(d) Element densities ρ_e corresponding to the approximate Heaviside function $\tilde{H}(\phi)$ of Fig. 10b.

Fig. 10 Examples of an exact and approximate Heaviside function and corresponding element-wise constant density distributions ρ_e of the LSF of Fig. 1a

level contour of the LSF $\phi = 0$. The only way to create larger regions with intermediate densities are 'islands' of material smaller than the resolution of the finite element discretization (Van Dijk et al. 2012).

Equation (17) can be evaluated either analytically or numerically. For an exact Heaviside formulation and depending on the parameterization of the LSF, (17) may be calculated analytically. This approach was adopted by Allaire et al. (2004) (personal communication), De Ruiter and Van Keulen (2004) and Van Dijk et al. (2012), who determined the material fractions using a triangular submesh. De Ruiter and Van Keulen (2004) used a semi-analytical approach to evaluate the sensitivities. A closed-form expression of the derivative of (17) to the nodal values of the LSF is presented in Van Dijk et al. (2012).

The integral in (17) can also be evaluated numerically,

$$\rho_e = \varepsilon + (1-\varepsilon)\frac{\sum_{j=1}^{n} w_j H(\phi(\boldsymbol{X}_j))}{\sum_{j=1}^{n} w_j}, \tag{18}$$

where w_j are the weight factors of the numerical integration (e.g., using standard Gauss quadrature). However, without special procedures such as aligned sub-domains, this type of numerical integration requires locally a large number of integration points $\boldsymbol{X}_j$ within each element cut by the zero-level contour of the LSF to accurately capture the discontinuity of the exact Heaviside function $H(\phi)$. Element densities defined by (18) are not differentiable with respect to the LSF.

Alternatively, (17) can also be integrated accurately using sub-domains aligned with the interface, similar to X-FEM (see Section 3.2). This approach results in a differentiable definition of the element densities that may be calculated using e.g., a semi-analytical approach.

When an approximate Heaviside formulation is used in (18), also a large number of closely spaced integration points are needed to capture the strong nonlinear behavior of the approximate Heaviside function $\tilde{H}(\phi)$ (Van Dijk et al. 2010). However, in this case the derivative of (18) with respect to the LSF is well-defined and can be calculated as,

$$\frac{\partial \rho_e}{\partial s_i} = \frac{1-\varepsilon}{\sum_{j=1}^{n} w_j} \sum_{j=1}^{n} w_j \tilde{\delta}(\phi(\boldsymbol{X}_j)) \frac{\partial \phi(\boldsymbol{X}_j)}{\partial s_i}, \tag{19}$$

where $\tilde{\delta}(\phi) = \partial \tilde{H}/\partial \phi$ is the approximate Dirac delta function and the term $\partial \phi(\boldsymbol{X}_j)/\partial s_i$ depends on the parameterization of the LSF.

Direct approach Alternatively, the density distribution can be defined by directly mapping the LSF into a density distribution. With some exceptions (e.g., Osher and Santosa 2001; Challis 2010), this approach is usually combined with an approximate Heaviside formulation (Liu et al. 2005; Liu and Korvink 2008; Pingen et al. 2010; Kawamoto et al. 2011; Luo et al. 2012). For instance Pingen et al. (2010) and Kawamoto et al. (2011) use the mapping,

$$\rho(\phi) = \varepsilon + (1-\varepsilon)\tilde{H}(\phi). \tag{20}$$

A point-wise mapped density distribution can be used directly in the weak form of the governing equations to solve integrals of the form (13). In this case, (20) is used at the integration points to approximate (13). In this manner, Liu et al. (2005) based their implementation on an approximate Heaviside formulation and a continuous density distribution. Similarly, Zhou and Zou (2008) and Luo et al. (2012) employ a meshless method for the structural analysis, where the density is used at the integration points of the background integration cells.

However, it is difficult to solve integrals such as (13) accurately due to the strong nonlinearity of the approximate Heaviside function. Therefore, Liu and Korvink (2008) used a mesh deformation technique to refine the discretization at the structural boundary to improve the accuracy of the mechanical model.

In its most simple form, the point-wise mapping (20) is used to control an element-wise constant density distribution (element densities), e.g., as,

$$\rho_e = (1-\varepsilon)\tilde{H}\left(\phi\left(\boldsymbol{X}_e\right)\right), \tag{21}$$

where $\boldsymbol{X}_e$ is the center of a finite element e (Pingen et al. 2010). In this case the derivative of the element density ρ_e can be consistently derived as,

$$\frac{\partial \rho_e}{\partial s_i} = (1-\varepsilon)\tilde{\delta}(\phi(\boldsymbol{X}_e))\frac{\partial \phi(\boldsymbol{X}_e)}{\partial s_i}. \tag{22}$$

This approach is easy to implement in an explicit LSM (Pingen et al. 2010).

An approximate Heaviside formulation uses information of the LSF from beyond the zero-level contour and, therefore, loses some of the crispness of a level-set-based design description. A direct mapping of the LSF into a density distribution using an approximate Heaviside is closely related to pure density-based TO and, in particular, to projection methods using *smoothed* Heaviside filters (Guest et al. 2004; Sigmund 2007; Guest 2009a, b; Wang et al. 2011), see also Section 7.4. Without measures to control the slope of the LSF near the interface (such as maintaining a signed-distance LSF), the LSF can become flat leading to large regions with intermediate density.

Using the simple direct mapping (21) in combination with an exact Heaviside formulation, an integer-valued material distribution is obtained. The element 'densities'

can only assume their extreme values $\rho_e = \varepsilon$ and $\rho_e = 1$ depending on the sign of the LSF in the single integration point of the elements. This approach is adopted by Challis (2010) in her MATLAB implementation of an LSM for structural optimization. A drawback of this approach is that the discrete material distribution is not differentiable with respect to the LSF. Therefore, a formulation using an approximate Heaviside function is often adopted. However, sensitivity information of level-set-based TO can also be derived from the continuum or variational problem instead of direct differentiation of the density distribution (Osher and Santosa 2001; Allaire et al. 2004; Challis 2010). This subject is discussed further in Section 4.

Similar to using (13) for the structural equilibrium equations, the density distribution ρ is often used to represent the material phases by scaling material properties (e.g., the Young's modulus), such as in the Ersatz material approach (Wang et al. 2003; Allaire et al. 2004) and SIMP (Bendsøe 1989; Zhou and Rozvany 1991; Rozvany et al. 1992). Other material interpolation schemes have been devised for pure density-based TO methods, including RAMP (Stolpe and Svanberg 2001), ECP (Yoon and Kim 2005) and EDS (Van Dijk et al. 2013, submitted), that can be used in level-set-based TO methods. A good choice of the relation between the local density and the structural model is not trivial and depends on the type of structural model used and the characteristics of the considered optimization problem (e.g., Swan and Kosaka 1997; Maute et al. 1998; Bendsøe and Sigmund 1999).

The use of an element-wise constant density distribution (either using the material fraction approach or the simple direct mapping) can result in non-smooth boundaries and/or regions of intermediate density, see Fig. 9c. This may have a negative effect on the accuracy of local quantities near the interface (e.g., stresses (Wei et al. 2010)) and boundary conditions at the interface (e.g., for fluid flows (Kreissl et al. 2011)), sometimes leading to physically unrealistic results and/or convergence problems of the analysis. Furthermore, a highly refined discretization may be needed to model curved surfaces with sufficient accuracy. The disadvantages associated with a density-based geometry mapping are shared with pure density-based TO methods. However, depending on the update procedure, the regions with intermediate densities in a level-set-based approach are often confined to the boundaries of a design and their size can be controlled.

Using an approximate Heaviside formulation results in a band of intermediate (element) densities $\varepsilon \leq \rho \leq 1$ where the LSF has intermediate values $-h < \phi < h$, see Fig. 10d. The size of the band of intermediate densities depends on the bandwidth h of the approximate Heaviside function and the local gradient of the LSF in the neighborhood of the boundary. For a signed-distance LSF the bandwidth h can be directly related to the size of the band of intermediate densities.

For a small bandwidth (depending on the steepness of the LSF), the intermediate values of the LSF $-h < \phi < h$ can be contained within one element. In this case, integrals over the material domain and boundary may be approximated with reasonable accuracy by replacing the Heaviside function $H(\phi)$ and Dirac delta function $\delta(\phi)$ in (8) and (10) with their approximate counterparts $\tilde{H}(\phi)$ and $\tilde{\delta}(\phi)$, respectively. A large bandwidth blurs the structural boundary but can have a smoothening effect on the structural responses and sensitivity fields (see Section 6).

Without any restriction on the gradient of the LSF the application of an approximate Heaviside function allows the occurrence of gray areas in TO (consider for instance the case $\phi = 0$, and therefore $\tilde{H} \approx \frac{1}{2}$ for a large area). Therefore, this type of approach is usually combined with a procedure to control the gradient of the LSF near the interface. This can be a reinitialization scheme to maintain the LSF as a signed-distance function (see Section 6.1) or a specific choice of LSF parameterization (see Section 2). You can also avoid large areas with intermediate densities using the same penalization techniques used in standard density-based TO (see Section 6.2).

Using an approximate Heaviside function, changes of the LSF within the bandwidth $-h < \phi < h$ have a direct effect on the densities and the structural response. Unless this is prevented by regularization techniques, new holes can nucleate in gradient-based LSMs where the LSF is within this bandwidth (see Section 4).

4 Update information

The LSF parameterization, the geometry mapping and the structural model control the behavior of the candidate designs as a function of the optimization variables $\boldsymbol{s}$. In this section, we discuss the different types of update information used in level-set-based TO methods.

Using an LSM, design changes are primarily governed by shape changes and are, therefore, mostly based on shape-sensitivity analysis. We distinguish between variational and parameter shape sensitivities (Sections 4.1 and 4.2, respectively). Sensitivity information can also be obtained using material parameter sensitivities, i.e., direct differentiation of the mechanical model (Section 4.3). To increase the topological complexity of designs, topological derivatives (Section 4.4) are often employed, see Fig. 11. In some cases the design updates are not based on sensitivity information but on heuristic criteria (Section 4.5). Certain types of sensitivities are often used in conjunction with specific update procedures.

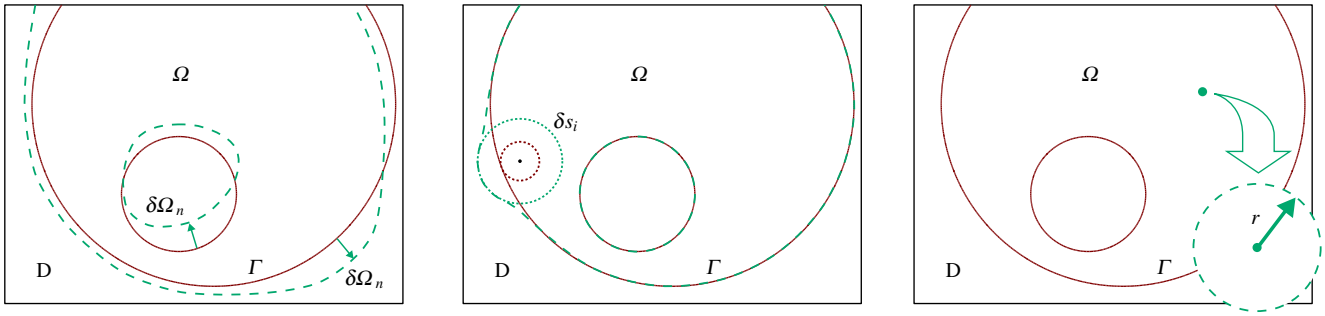

(a) A boundary variation $\delta\Omega_n$. (b) A parameter variation δs_i. (c) A topological variation with radius $r \to 0$.

Fig. 11 Boundary, topological and parameter variations

In general, a response function (i.e. objective or constraint) in a structural optimization depends on the shape and topology of the material domain Ω and a state variable such as the displacement $\boldsymbol{u}$. To clarify the discussion in this section, we define a general response function R as,

$$R(\Omega, \boldsymbol{u}(\Omega)) = \int_\Omega r_\Omega(\boldsymbol{u}) dV + \int_\Gamma r_\Gamma(\boldsymbol{u}) dS. \tag{23}$$

For example, the integrands for the compliance of a structure without body forces can be written as $r_\Omega = 0$ and $r_\Gamma = \boldsymbol{t} \cdot \boldsymbol{u}$, where $\boldsymbol{t}$ is the external load on the boundary.

The response function R depends explicitly on the material domain Ω via the integration domains Ω and Γ and implicitly via the state variable $\boldsymbol{u}$. The state variable is a function of the material domain $\boldsymbol{u} = \boldsymbol{u}(\Omega)$, because the state (equilibrium) equations are defined over the material domain Ω. In the sensitivity analysis of TO methods, the dependence of the response function R on the state variable $\boldsymbol{u}$ is typically incorporated using an adjoint approach, rather than direct differentiation of the state equation (Bendsøe and Sigmund 2003).

In this section, we focus on the direct dependency of the response function R on the material domain Ω, assuming a generic form of the state equations. Apart of the volume and boundary integrals in (23), a response function R can also involve explicit expressions involving the LSF (e.g., penalization of the norm of the gradient of the LSF, see Section 6.1).

4.1 Variational shape sensitivities

Most LSMs base the evolution of the LSF on shape-sensitivity information, e.g., Osher and Santosa (2001), Wang et al. (2003), Allaire et al. (2004), Wang and Wang (2006b), Luo et al. (2008a, b), Myśliński (2008) and Challis and Guest (2009). Shape-sensitivity analysis, see e.g., Sokołowski and Zolésio (1992) is concerned with the sensitivity of a response function to changes of the shape of the material domain, see Fig. 11a. Only infinitesimal changes of the boundary in the normal direction to the boundary cause shape changes of the material domain (Allaire et al. 2004). Therefore, shape sensitivities are only a function of normal boundary variations indicated with $\delta\Omega_n$, see Fig. 11a.

In the implementation of shape sensitivity analysis we distinguish between variational and parametrized (also called discrete) shape sensitivities. Rather than first discretizing the governing equations of the optimization problem, *variational* shape sensitivities are derived from the variational expression of the optimization problem and the state equations. Subsequently, the sensitivity equation in variational form is discretized independently from the responses (Van Keulen et al. 2005). Variational shape sensitivity fields are exclusively used in update procedures based on the Hamilton–Jacobi (HJ) (see Section 5.1). More information on the (derivation of) shape sensitivities can be found in the textbook of Sokołowski and Zolésio (1992) and the review by Burger and Osher (2005). On the other hand, parameter shape sensitivities relate the shape sensitivity directly to the independent optimization variables $\boldsymbol{s}$, based on the discretized LSF and numerical mechanical model. They are often used in update procedures based on mathematical programming (see Section 5.2).

A first-order variation of the response function δR due to a normal variation of the boundary $\delta\Omega_n$ results in an equation of the form,

$$\delta R = \int_\Gamma \mathrm{d}_S R \, \delta\Omega_n dS, \tag{24}$$

where $\mathrm{d}_S R$ is called the shape gradient of the response function R that depends on the definition of the response function (i.e., $r_\Omega(\boldsymbol{u})$ and $r_\Gamma(\boldsymbol{u})$). For example, in the case of the compliance (without body forces), the shape gradient

can be written as $\mathrm{d}_S R = -\boldsymbol{\epsilon}(\boldsymbol{u}) : \mathbf{C} : \boldsymbol{\epsilon}(\boldsymbol{u})$ on the traction-free boundaries of the structure (for a derivation see Allaire et al. 2004).

Similarly to shape optimization, e.g., Sokołowski and Zolésio (1992) and Choi and Kim (2005), in level-set-based TO the process of changing the shape of the material domain Ω is often viewed as a pseudo-dynamic process where the material domain is evolving in pseudo time τ representing the design iterations (see Section 5.1). The 'deformation' of the material domain at pseudo time $\tau = 0$ can be represented by a normal 'design' velocity field v_n as (Choi and Kim 2005),

$$\boldsymbol{X}_\tau = \boldsymbol{X} + \tau v_n \boldsymbol{n}, \tag{25}$$

where $\boldsymbol{n}$ is the normal vector to the boundary. Based on (24), we construct a normal velocity field v_n that describes the motion of a point on the boundary Γ in the optimization process. This is usually done by replacing the variation of the boundary $\delta\Omega_n$ in (24) with the normal velocity field v_n and choosing it such that it corresponds to a descent-direction of the optimization problem (Allaire et al. 2004).

In shape optimization, the velocity field v_n needs to be extended in the interior of the material domain Ω to maintain the regularity of the finite element mesh distribution as much as possible. For velocity-based LSMs the velocity field needs to be defined at least on a band around the interface to maintain the regularity of the LSF near its zero-level contour (Sethian 1999; Osher and Santosa 2001; Allaire et al. 2004).

However, there is no unique way to define the velocity v_n in the interior of the material domain Ω (Choi and Kim 2005). The following kinds of velocity field extensions have been proposed for different purposes: the *normal*, the *natural* and *Helmholtz* velocity extension. The velocity field v_n should be constructed to drive the optimization process towards an optimum and vanish on the boundary Γ when the optimality conditions are satisfied. Depending on their implementation, velocity extensions can be closely related to sensitivity regularization (see Section 6.3).

Normal velocity extension The velocity field can be extended from the material boundary to be constant in the normal direction (Sethian and Wiegmann 2000, Wang et al. 2004, Wang and Wang 2004a, b; Yulin and Xiaoming 2004a; Zhuang et al. 2007; Rong and Liang 2008). Analogously to maintaining a regular mesh in shape optimization, the goal of such a velocity extension in LSMs is to maintain a smooth LSF. When the LSF is a signed-distance function, theoretically a normal velocity extension maintains this property (Sethian and Wiegmann 2000). Therefore, shape-sensitivity-based LSMs using a normal velocity extension cannot create new holes in the interior of the material domain. In practice, the LSF deviates from the signed-distance function due to the discretization and finite updates of the LSF. To extend the velocity field from the boundary into the design domain an additional PDE needs to be solved.

Natural velocity extension For LSMs that model the void phase as a weak material, the shape gradient $\mathrm{d}_S R$ often involves quantities that are defined not only on the boundary Γ but everywhere in the design domain D (e.g., $-\boldsymbol{\epsilon}(\boldsymbol{u}) : \mathbf{C} : \boldsymbol{\epsilon}(\boldsymbol{u})$ for compliance). In this case, a velocity field can be constructed from the shape gradient $\mathrm{d}_S R$ and evaluated everywhere in the design domain D. This is referred to as a natural velocity extension (Osher and Santosa 2001; Wang et al. 2003; Allaire et al. 2004; Kwak and Cho 2005; He et al. 2007; Allaire and Jouve 2008; Luo et al. 2008b; Challis and Guest 2009). This type of velocity extension does not require solving an additional PDE. When the LSF in the interior of the material domain is allowed to move independently of the boundary (e.g., no signed-distance reinitialization), then the application of a natural velocity extension can lead to the incidental nucleation of new holes in the interior of the material domain (Luo et al. 2008b).

Hilbertian velocity extension De Gournay (2006) proposes a Hilbertian velocity extension. This extension regularizes the velocity by introducing a convenient scalar product for the computation of the descent direction. This approach is based on ideas that were introduced earlier by Burger (2003). The Hilbertian velocity extension adopts a scalar product based on a Hilbertian structure and allows treatment of problems that are not Fréchet differentiable but whose directional derivatives do exist. In this case, a semi-definite programming problem needs to be solved for the construction of the velocity field. No new holes can be generated with this extension.

Helmholtz extension Yamasaki et al. (2011) use a velocity extension based on the Helmholtz equation following the approach of Lazarov and Sigmund (2011). The velocity field on the boundary is smoothed over the design domain. The Helmholtz PDE can be easily solved using a finite element discretization. Since this type of velocity extension relates the velocity to the shape sensitivity on the boundary new holes cannot be generated.

Shape-sensitivity analysis does not provide information on topological changes. However, using a velocity field based on variational shape sensitivities for the update of the LSF can lead to a reduction of topological complexity (e.g., merging and disappearing holes). In this case, an improvement of the design in terms of performance and/or feasibility is not guaranteed. In fact, topological changes

only occur incidentally due to the finite step size of the level-set updating algorithm.

Using a natural velocity extension holes may appear inside the material domain, depending on the update procedure (see Section 5.1) and the applied regularization (see Section 6) (Luo et al. 2008b). However, the shape gradient is constructed for boundary changes and not for hole nucleation inside the material domain. The creation of holes is again incidental and does not guarantee improving the design.

However, in practice these topological changes do often result in increased performance and/or feasibility. Extended velocity fields are commonly used in LSMs in combination with a density-based geometry mapping. For this type of approach *naturally* extended velocity fields can be similar to the sensitivity fields used in density-based TO methods. This subject is further discussed in Section 7.4. The level of similarity depends on the discretization of the velocity field and the design parameterization.

The variational shape sensitivities used in LSMs are not necessarily numerically consistent with the mechanical model. These inconsistencies can have either positive or negative effects on the optimization process. This subject is revisited in more detail in Section 7.1.

4.2 Parameter shape sensitivities

In the derivation of parameter (or parametrized) shape sensitivities, the LSF is first discretized and subsequently the shape sensitivities are related directly to the optimization variables $\boldsymbol{s}$ (Belytschko et al. 2003; Liu et al. 2005; Liu and Korvink 2008; Luo et al. 2008c; Wei et al. 2010; Ho et al. 2011; Van Dijk et al. 2012).

Variations of an optimization variable δs_i are directly related to a boundary variation $\delta\Omega$, see Fig. 11a. The boundary of the material domain Γ is characterized by the zero-level contour of the LSF $\phi = 0$. Substituting the most common parameterization of the LSF $\phi = \sum_i N_i s_i$ and taking the variation of the contour, we obtain,

$$\sum_i N_i \delta s_i + \nabla\phi \cdot \delta\Omega = 0, \tag{26}$$

where $\delta\Omega$ is the vectorial variation of the boundary. Using (1), the outward normal to the boundary is given by,

$$\boldsymbol{n} = \frac{-\nabla\phi}{\|\nabla\phi\|}. \tag{27}$$

Due to the inner product in (26), variations of the optimization variables δs_i only lead to variations of the boundary in the normal direction $\delta\Omega_n \boldsymbol{n}$. Substituting $\delta\Omega_n \boldsymbol{n}$ for the boundary variation $\delta\Omega$ in (26) and using (27), we can write the normal boundary variation $\delta\Omega_n$ in terms of variations of the optimization variables δs_i as,

$$\delta\Omega_n = \sum_i \frac{N_i \delta s_i}{\|\nabla\phi\|}. \tag{28}$$

Liu and Korvink (2008), Luo et al. (2008c), Wei et al. (2010), Ho et al. (2011) and Van Dijk et al. (2012) use this relation to link the shape sensitivities of the form (24) to the individual optimization variables of the parameterization of the LSF. Substituting (28) in (24) we obtain the parametrized or discrete shape sensitivities $\partial R/\partial s_i$ as,

$$\frac{\partial R}{\partial s_i} = \int_\Gamma \mathrm{d}_S R \, \frac{N_i}{\|\nabla\phi\|} dS. \tag{29}$$

Depending on the geometry mapping, the evaluation of this boundary integral can be difficult, because the boundary is not explicitly parametrized. For the special case of a piecewise linear interpolation of the LSF and piecewise constant shape gradient, Van Dijk et al. (2012) evaluate this boundary integral analytically. The boundary integrals can also be calculated using numerical quadrature (Luo et al. 2008c). Similarly, Maute et al. (2011) and Makhija and Maute (2013, submitted) evaluate this boundary integral in an X-FEM-based approach using numerical integration, where the boundaries of the integration sub-domains are aligned with the zero-level contour of the LSF. In this manner, parameter shape sensitivity analysis can be implemented consistently with the discretized optimization problem and is particularly well suited for use with mathematical programming methods (see Section 5.2).

Alternatively, (29) can be approximated by replacing the boundary integral with a volume integral using an approximate Dirac delta function (see (10) in Section 3.3) (Belytschko et al. 2003; Luo et al. 2007, 2009b; Luo and Tong 2008). Approximations of (29) reduce the accuracy of the design sensitivities. This may lead to oscillations in the optimization process and a decreased performance of mathematical programming methods (see Section 7.1).

Rather than evaluating a boundary integral of the form (29), a semi-analytical approach was adopted in the works of De Ruiter and Van Keulen (2004) and Van Miegroet and Duysinx (2007). For a small number of optimization variables even global finite differencing can be used to obtain the sensitivities of the response functions with respect to the optimization variables (Van Miegroet et al. 2005).

The magnitude of the gradients of the response function in (29) heavily depends on the norm of the spatial gradients of the LSF. For a flat LSF the sensitivities only provide accurate predictions of the response functions for small variations of the LSF. This can cause scaling problems and ill-conditioning of the optimization process. To avoid these

problems additional requirements can be imposed on the LSF (see Section 7.1).

4.3 Material parameter sensitivities

For a density-based geometry mapping employing the simple direct mapping of the LSF to an element density field using an approximate Heaviside formulation (21), the sensitivity of a response function R with respect to an optimization variable s_i can be obtained by the chain rule (Pingen et al. 2010; Kawamoto et al. 2011; Kreissl et al. 2011),

$$\frac{\partial R}{\partial s_i} = \sum_e \frac{\partial R}{\partial \rho_e} \frac{\partial \rho_e}{\partial s_i}, \tag{30}$$

where the term $\partial \rho_e / \partial s_i$ involves the approximate Heaviside $\tilde{H}(\phi)$.

In contrast to the shape sensitivities discussed earlier, the sensitivities $\partial R / \partial s_i$ are similar to the sensitivities used in density-based TO methods using a Heaviside projection scheme (Guest 2009b; Wang et al. 2011). A significant difference is that the sensitivities are only non-zero near the material boundaries.

4.4 Topological derivatives

Shape sensitivities only provide information to alter the boundary of the material domain. For the interior of the material domain, topological sensitivities provide information on changes of response functions due to the perforation of the material domain by an infinitesimal hole (Eschenauer et al. 1994; Schumacher 1995; Sokołowski and Żochowski 1999; Céa et al. 2000; Garreau et al. 2001), see Fig. 11b. The topological gradient $\mathrm{d}_{\mathcal{T}} R$ is defined as the change of a response function R due to the insertion of a (void) sphere B as its radius approaches zero,

$$\mathrm{d}_{\mathcal{T}} R = \lim_{r \downarrow 0} \frac{R(\Omega \setminus B(r)) - R(\Omega)}{|B(r)|}, \tag{31}$$

where $|\cdot|$ is a measure of the volume (Sokołowski and Żochowski 1999; Garreau et al. 2001). A topological derivative depends on the shape of the hole B, the boundary conditions imposed on the boundary of the hole Γ_B and the spatial dimensions (Sokołowski and Żochowski 1999, 2001; Garreau et al. 2001). Two types of topological derivatives can be found in the literature, (i) topological derivatives based on shape derivatives of an infinitesimal hole (Céa et al. 2000; Novotny et al. 2003; Burger et al. 2004; He et al. 2007) and (ii) topological derivatives based on an asymptotic expansion of the objective functional (Sokołowski and Żochowski 1999; Garreau et al. 2001; Sokołowski and Żochowski 2001), where the latter definition is most often adopted, see e.g., Amstutz and Andrä (2006), Norato et al. (2007) and Allaire and Jouve (2008).

Topological gradient information is frequently employed to systematically nucleate holes in the interior of the material domain, e.g., Burger et al. (2004), Allaire et al. (2005), Yulin and Xiaoming (2004a), Fulmański et al. (2007, 2008), Myśliński (2008) and Challis and Guest (2009). It can be used to periodically insert a new a hole in a separate step of the optimization process (Yulin and Xiaoming 2004a; Allaire et al. 2005; Fulmański et al. 2007, 2008; Myśliński 2008; Challis and Guest 2009).

Alternatively, Burger et al. (2004) include an additional term in the HJ equation (see Section 5.1) based on the topological derivative such that new holes can continuously nucleate in the interior of the material domain. The rate of convergence of the optimization process depends on these hole generation mechanisms (Allaire et al. 2005). More iterations are necessary because whenever a new hole is formed, essentially a new optimization problem is generated.

It is also possible to use exclusively topological gradient information to drive the LSF. Iso-contours of the topological gradient field, based on a material removal rate, were used to define the material domain by Céa et al. (2000), Garreau et al. (2001) and Norato et al. (2007). These approaches can be viewed as LSMs where the LSF is defined as the topological derivative field itself. When the topological gradient field becomes stationary, an optimum has been reached. Céa et al. (2000) and Garreau et al. (2001) formulate this strategy as an irreversible approach where (material) elements are only removed. Norato et al. (2007) use a slightly different approach based on a density distribution allowing the addition of material. Fully bi-directional LSMs based on topological derivatives were devised by Amstutz and Andrä (2006) and He et al. (2007).

Topological derivatives are closely related to shape sensitivities (Céa et al. 2000) and density sensitivities (Amstutz 2011). More information on this subject can be found in Section 7.4. The relation between topological derivatives, shape sensitivities and density derivatives may be an interesting subject for future research.

4.5 Non-sensitivity information

Relatively few LSMs base an update of the LSF on non-sensitivity information. One of the first LSMs, proposed by Sethian and Wiegmann (2000), was an evolutionary approach involving a heuristic stress-based update criterion. In their approach a normal boundary velocity was defined based on the Von Mises stress at the boundary (see Section 4.1). New holes could be introduced in the interior of the structure using iso-contours of the stress field.

5 Update procedure

In most LSMs design sensitivities are used to update the LSF. The associated update procedure, including techniques for handling move limits and constraints, strongly influences the efficiency and convergence rate of the optimization process and as well as the final result. In some cases regularization techniques are integrated into the update procedure of the LSF. We distinguish between two major classes of update strategies. The first class treats the optimization process as a quasi-temporal process in which the boundaries of the material domain are advanced based on a velocity field (Section 5.1). The second class of methods are based on mathematical programming (Sections 5.2–5.4). In this section the different types of update procedures are discussed.

5.1 Hamilton–Jacobi equation

Traditionally, the evolution of the LSF in the optimization process is governed by the Hamilton–Jacobi (HJ) equation. In level-set-based TO, this partial differential equation describes the motion of the material interface due to a design velocity field $\boldsymbol{v}$. In its original form, the HJ equation is first-order and models convection only,

$$\frac{\partial \phi}{\partial \tau} + \nabla \phi \cdot \boldsymbol{v} = 0, \tag{32}$$

where τ denotes a pseudo time that represents the iterations in the optimization process. At the optimum the velocity field vanishes and the LSF stagnates. As the normal to the zero-level contour is related to the gradient of the LSF by (27) (depending on the definition of the material domain (1)), the HJ equation (32) can be simplified as follows (Osher and Fedkiw 2003),

$$\frac{\partial \phi}{\partial \tau} - v_n \|\nabla \phi\| = 0, \tag{33}$$

where $v_n = \boldsymbol{v} \cdot \boldsymbol{n}$ denotes the normal velocity field. Subsequently, we focus on the HJ equation in form of (33) as this formulation is predominantly used in the context of TO. For a more mathematical discussion, we refer the reader to the survey by Burger and Osher (2005) and the text books by Sethian (1999) and Sethian (2001) and Osher and Fedkiw (2003).

While the goal of the HJ equation is to describe the evolution of the material interface, i.e. the zero level set, the velocity field v_n in (33) needs to be defined over the entire design domain or at least in a band around the boundaries (Burger and Osher 2005). The velocity v_n on the boundary is typically derived from variational shape sensitivity analysis (see Section 4.1). Approaches for expanding the velocity field into the domain are also summarized in Section 4.1.

For a given velocity field, the numerical solution of (32) and (33) requires some form of stabilization to avoid node-to-node oscillations and to limit the magnitude of the spatial gradients of the LSF (Sethian 1999, 2001). In general, such stabilization schemes introduce numerical diffusion and smoothen the LSF. Furthermore, the LSF is typically re-initialized to a signed-distance function (see Section 6.1) to avoid that the LSF becomes too flat or too steep, both of which may lead to convergence issues (Allaire et al. 2004). The original formulation of the HJ equation can be augmented by explicitly adding diffusive and reaction terms.

From an optimization point of view, the time-discretized HJ equation (32) can be interpreted as an unconstrained primal method, advancing the LSF values in the direction $\boldsymbol{n}$ by updating the LSF values with local step size $\Delta\phi = v_n \|\nabla\phi\| \Delta\tau$. In particular, when the LSF remains a signed-distance function throughout the optimization process ($\|\nabla\phi\| = 1$), the relation to primal methods is clear: $\Delta\phi = v_n \Delta\tau$ (Abe et al. 2007; Yamasaki et al. 2010a). However, adding diffusion and reaction terms and numerical stabilization techniques introduce a form of intrinsic regularization, thus rendering the HJ equation an interesting alternative to conventional optimization methods. Subsequently, we discuss various formulations of the resulting convection-diffusion equations and numerical schemes for solving the HJ equation.

Generalized HJ equation In addition to the convective term in (33), diffusive and reaction terms have been introduced to stabilize numerical solution, regularize the LSF and nucleate new holes,

$$\frac{\partial \phi}{\partial \tau} - v_n \|\nabla \phi\| - \mathcal{D}(\phi) - \mathcal{R}(\phi) = 0, \tag{34}$$

where $\mathcal{D}$ represents a diffusive operator and $\mathcal{R}$ is a reaction term acting on the LSF values. Note that when diffusion is included in the generalized HJ equation, (34) becomes a second-order differential equation and is, strictly speaking, no longer a HJ equation (Osher and Fedkiw 2003; Burger and Osher 2005).

Diffusion Adding diffusion in general eases the numerical treatment of the HJ equation, smooths the LSF and reduces the dependency of the optimization results on the discretization of the LSF. For a broader discussion of LSF regularization methods the reader is referred to Section 6.1. If the diffusion term dominates over the convective term in (34), stabilization methods are typically not needed for numerically solving the generalized HJ equations.

Linear isotropic diffusion was proposed by, e.g., Liu et al. (2005) and Liu and Korvink (2008),

$$\mathcal{D} = c_{\text{iso}} \nabla \cdot (\nabla \phi), \tag{35}$$

where c_{iso} is a scalar diffusion coefficient that controls the strength of the diffusion. This approach is also referred to as Tikhonov regularization (Tikhonov et al. 1995), see Section 6.1.

The concept of linear isotropic diffusion can be expanded onto linear anisotropic diffusion, replacing the scalar diffusion coefficient with a diffusion tensor $\mathbf{C}$. In the context of level-set-based TO, Yamada et al. (2010), Lim et al. (2011) and Otomori et al. (2011) introduce such an energy term into a diffusion-reaction evolution equation to regularize the level-set function. Introducing anisotropic diffusion leads to different length-scales in different spatial directions (Yamada et al. 2010).

Alternatively to linear diffusion, diffusion in streamline direction can be added to control the mean curvature of the LSF, e.g., Wang et al. (2003), Allaire et al. (2004), Wang and Wang (2004b), Chen et al. (2008), Luo et al. (2008a), Rong and Liang (2008) and Wei and Wang (2009),

$$\mathcal{D} = c_{\text{sld}} \nabla \cdot \left(\frac{\nabla \phi}{\|\nabla \phi\|} \right), \tag{36}$$

where c_{sld} is yet another diffusion coefficient. As the gradient of the LSF $\nabla\phi$ is related to the normal $\boldsymbol{n}$ by (27), this can be written as $\mathcal{D} = -\nabla \cdot \boldsymbol{n}$ and is also referred to as mean curvature flow (see Section 6.1) (Osher and Fedkiw 2003; Burger and Osher 2005). Isotropic and streamline diffusion can be combined (Duan et al. 2008).

Reaction The reaction term in the generalized HJ equation can be used to introduce source and sink terms within the solid domain to nucleate new holes. Burger et al. (2004), He et al. (2007), Challis and Guest (2009) and Challis (2010) included reaction terms derived from the topological derivative (see Section 4.4).

Departing from the original concept of the HJ equations, Yamada et al. (2010), Lim et al. (2011) and Otomori et al. (2011) omitted the convective term and only use a reaction term to drive the evolution of the LSF. As the reaction term exists on the entire design domain and the concept of shape derivatives is not used, this approach is no longer considered an LSM in the traditional sense (see also Section 7.4).

Solution methods To update the LSF, either the original HJ equation (33) or generalized form (34) needs to be discretized in space and pseudo time and the resulting discrete system solved numerically. The numerical treatment of the HJ equation is non-trivial due to stability issues. In the case that the convective term is dominant, node-to-node oscillations may occur. This phenomenon is well known from convective problems, for example in computational fluid dynamics, and affects all discretization methods, such as finite difference, finite volumes, and finite elements (Brooks and Hughes 1982; Hirsch 2007). These spurious node-to-node oscillations can be suppressed by introducing numerical dissipation in streamline direction using upwinding. Advancing the LSF in pseudo time with explicit schemes, stability conditions limiting the maximum step size in dependency of the mesh size need to be obeyed in addition (Osher and Fedkiw 2003).

Depending on the discretization method, upwinding can be realized in various forms (e.g., Lyra and Morgan 2000a, b, 2002). Many authors have used efficient finite-difference upwinding schemes for structured grids (Osher and Santosa 2001; Wang et al. 2003; Allaire et al. 2004; Wang and Wang 2006a; He et al. 2007; Allaire and Jouve 2008; Challis and Guest 2009). More general upwinding schemes need to be applied for unstructured grids, typically used for arbitrarily shaped design domains (Cecil et al. 2004). Alternatively, Xing et al. (2010) used a streamline diffusion finite element method (SDFEM) to solve the HJ equation on structured and unstructured meshes.

The semi-discrete form of the HJ equation can be advanced in pseudo time using explicit (e.g., Wang et al. 2003; Allaire et al. 2004), semi-implicit (e.g., Luo et al. 2008a; Mohamadian and Shojaee 2012) or fully implicit time marching schemes. The latter typically leads to a substantially increased numerical burden. Due to their algorithmic simplicity, explicit methods, such as an Euler forward scheme, are frequently used (Osher and Santosa 2001; Wang et al. 2003; Allaire et al. 2004; Wang and Wang 2006a; He et al. 2007; Allaire and Jouve 2008; Challis and Guest 2009). In this case, however, the maximum time step $\Delta\tau$ is limited by the Courant–Friedrichs–Lewy (CFL) condition (Osher and Fedkiw 2003). For an LSF discretized on a structured grid the CFL conditions require that the time step satisfies,

$$\Delta\tau \max(v_n) \leq h, \tag{37}$$

where h is the grid spacing. As the accuracy of explicit methods is generally poor, the pseudo time step size should be much smaller than the stability limit, i.e. $\Delta\tau \max(v_n) \ll h$. In this case, multiple time steps are necessary to achieve reasonable shape changes.

To relax the CFL condition but avoid the numerical complexity and computational costs of an implicit scheme, the HJ equation can be advanced in time by semi-implicit methods using an operator splitting approach. Operator splitting can be applied to either the different terms of the HJ equation (34), solving a sequence of convection and diffusion-reaction equations, or to the individual spatial dimensions, solving multiple one-dimensional problems (Yanenko 1971; Marchuk 1990). The latter approach was adopted by Luo et al. (2008a), Wei and Wang (2009) and Mohamadian and Shojaee (2012) using an Additive Operator Splitting (AOS) scheme to solve a diffusion dominated generalized HJ equation.

Using a semi-Lagrangrian approach (Strain 1999), Allaire et al. (2011) solve a linear advection equation (32) by the method of characteristics (Pironneau 1989).

Constraints and velocity fields The main purpose of the velocity field in the HJ equation is to advect the zero-level iso-contour of the LSF toward the optimum geometry while maintaining a regular LSF in the entire design domain. In the absence of design constraints, the extended design sensitivity fields can be used directly to construct the HJ velocity field. In the presence of design constraints, the constrained optimization problem needs to be transformed into an unconstrained one, e.g., via penalty or augmented Lagrange multiplier formulations. This may significantly hamper the convergence of the optimization process, in particular in the presence of a large number of constraints.

Often penalty formulations are used to reformulate the constrained optimization problem into an unconstrained one (Wang et al. 2003; Allaire et al. 2004; Amstutz and Andrä 2006; Chen et al. 2010). The associated penalty factors are sometimes referred to as fixed Lagrange multipliers (Wang et al. 2003; Allaire et al. 2004). This approach cannot enforce constraints exactly and results depend on the chosen penalty factors.

In an augmented Lagrangian formulation, the Lagrange multipliers are adapted iteratively based on the constraint value (Belytschko et al. 2003; De Ruiter and Van Keulen 2004; Luo et al. 2008c; Challis 2010) or using a constraint projection method (Osher and Santosa 2001; Wang and Wang 2004a; Yulin and Xiaoming 2004b; Liu et al. 2005; Abe et al. 2007; Challis and Guest 2009; Van Dijk et al. 2012). Furthermore, constraint violation can be dealt with using a separate return mapping (Osher and Santosa 2001; Rong and Liang 2008) or by augmenting the Lagrange multipliers with a penalty term, meeting the constraints exactly (Yulin and Xiaoming 2004a; Zhuang et al. 2009; Van Dijk et al. 2012).

Regularization In the case of the original HJ equation (33) only the numerical diffusion due to the stabilization techniques smooths the LSF. Introducing additional diffusive terms allows for an additional control over the smoothness of the LSF (see Section 6.1). If diffusion is added mainly to stabilize equations, the diffusion coefficients are derived from numerical stability criteria. However, the appropriate strength of the diffusive terms relative to the convection is problem dependent. While increasing diffusion tends to generate smooth geometries and suppresses sharp corners, in particular isotropic diffusion may lead to overly flat LSFs and may require frequent reinitialization. In addition, as the influence of diffusive terms on update scheme increases, the influence of the sensitivity information on the velocity field is reduced, affecting the convergence of the optimization process (see also Section 7.1). Therefore, the diffusion coefficients in (35) and (36) need to be chosen carefully (see also Section 6.1).

Updating the LSF via the original or generalized HJ equation provides an interesting approach to integrate regularization methods and hole nucleation into the optimization scheme. However, the overall approach is rather complex and requires tuning a large number of algorithmic steps for particular optimization problems.

5.2 Mathematical programming

A broad range of mathematical programming methods have been applied to density-based TO, such as Sequential Quadratic Programming (SQP), the Method of Moving Asymptotes (MMA (Svanberg 1987; Bruyneel et al. 2002)), CONvex LINearization approximations (CONLIN (Fleury and Braibant 1986)) and Quadratic Approximations (Groenwold and Etman 2010). Recently, the use of mathematical programming has gained popularity in the level-set-based TO field as well (Wang and Wang 2006b; Luo et al. 2008c; Maute et al. 2011; Otomori et al. 2011; Van Dijk et al. 2012).

One of the most basic gradient-based mathematical programming approaches is the steepest descent method (SDM). This type of approach has been used in the work of Van Dijk et al. (2012). However, more sophisticated approaches should be preferred. Haber (2004) employ SQP and Van Miegroet and Duysinx (2007) use CONLIN to significantly improve the convergence rate. The vast majority of authors solve level-set-based TO problems using MMA (Norato et al. 2004; Van Miegroet et al. 2005; Frei et al. 2007; Luo et al. 2007, 2009b; Luo and Tong 2008; Pingen et al. 2010; Kreissl et al. 2011; Maute et al. 2011). Most LSMs combine MMA with an RBF-based parameterization of the LSF, e.g., Norato et al. (2004), Luo et al. (2007) and Kreissl et al. (2011). However, MMA can also be applied to a FEM-based parameterization (Maute et al. 2011) and geometric shapes (Van Miegroet et al. 2005).

Mathematical programming requires sensitivities of the objective and constraints with respect to the optimization variables $\boldsymbol{s}$ (see Section 4.2). Similar to density-based TO, numerically consistent sensitivities, i.e., the exact derivatives of the numerically obtained objective and constraints with respect to the optimization variables, are in general most effective (see Section 7.1). For instance, Van Miegroet et al. (2005) and Pingen et al. (2010) use MMA in combination with parameter sensitivities. However, numerically inconsistent sensitivities as a result of regularization (see Section 6.3) or approximations are not necessarily problematic (see Section 7.1). For instance, Luo et al. (2007) use

approximated sensitivity information in combination with MMA to solve compliant mechanism design problems.

Sophisticated step size selection, constraint handling and move limit strategies are included in advanced mathematical programming methods. Their implementations have been optimized for speed and efficiency and can be used to solve optimization problems efficiently. In particular, MMA is promising for suppressing oscillations in the optimization process using an adaptive move limit strategy.

5.3 Optimality Criteria method

The Optimality Criteria (OC) method is a fixed-point approach to design problems, where the optimality conditions of a (single-constraint) optimization problem are used to update the optimization variables (Bendsøe and Sigmund 2003). This method has been used extensively in density-based TO (Bendsøe and Kikuchi 1988; Rozvany and Zhou 1991; Zhou and Rozvany 1991; Rozvany et al. 1992, 1995; Bendsøe and Sigmund 2003). It can also be used in a level-set-based approach (Céa et al. 2000; Garreau et al. 2001; Belytschko et al. 2003; Norato et al. 2007; Luo et al. 2008c).

For a single volume-constrained optimization problem (for instance compliance minimization) the optimality conditions can be written as,

$$\delta f + \lambda \delta g = 0, \tag{38}$$

where $\lambda \geq 0$ is the Lagrange multiplier associated with the volume constraint and δf and δg are variations of the objective and the volume constraint, respectively. Using (38) an update rule can be devised to improve the objective while satisfying the volume constraint exactly. The Lagrange multiplier λ is (iteratively) chosen such that the new design exactly satisfies the volume constraint. Furthermore, the update rule typically involves a move limit and numerical damping to improve the convergence behavior (Bendsøe and Sigmund 2003) and can be related to sequential approximate optimization with quadratic intervening variables (Groenwold and Etman 2008).

Belytschko et al. (2003) use the parameter derivatives in an OC approach with numerical damping. They use bisection to find an appropriate value for the Lagrange multiplier λ associated with the volume constraint. Luo et al. (2008c) use a similar approach where the LSF is discretized by RBFs.

Céa et al. (2000) and Garreau et al. (2001) use a topological gradient field as the LSF in an evolutionary method based on optimality conditions. Based on a material-removal rate, the volume is decreased in every iteration of the optimization process until a desired volume is obtained. The iso-contour of the topological derivative field corresponding to a required volume is used for the definition of the material domain. Similarly, Céa et al. (2000), Garreau et al. (2001) and Norato et al. (2007) use a topological gradient field in an approach where the material domain can also expand.

The OC method is an efficient way to update the optimization variables. The algorithm assumes regularity/monotonicity of the objective and constraint. For problems satisfying this assumption, such as compliance in density-based TO, OC methods converge well, avoiding oscillations of the optimization variables. However, for non-monotonic objectives this approach may not work as well.

5.4 Global search and gradient-free methods

De Ruiter and Van Keulen (2004) explored a Genetic Algorithm (GA) to find optimal geometries described by RBFs. Global search algorithms such as GA are applicable when there are relatively few optimization variables (Sigmund 2011). In this case they can be used to search for a global solution avoiding local minima. However, most level-set-based TO methods involve a large number of optimization variables which render global search algorithms too computationally expensive.

Gomes and Suleman (2006) apply a derivative-free trust-region method to a level-set-based TO method using a spectral approximation of the LSF. This approach is also computationally expensive, especially when a large number of optimization variables is involved.

6 Regularization

Regularization is often added to LSMs to obtain a well-posed optimization problem, remove numerical artifacts from the final results, improve the convergence behavior and avoid convergence to local minima with poor performance. Furthermore, regularization techniques are often employed to control geometrical properties of the resulting designs (e.g., boundary smoothness, feature size and topological complexity). Below we describe the goals of typical regularization techniques. Note most of these techniques result in multiple regularization effects and, therefore, may serve multiple goals.

Establishing uniqueness of the LSF In an LSM, the shape and topology of a design only depends on the zero-level contour of the LSF. Therefore, the LSF in the interior of the material domain and the gradient of the LSF on the boundary of the optimal design are not uniquely defined (Haber 2004). This issue is particularly important because the gradient of the LSF along the zero-level contour has a large

influence on the convergence rate of the optimization process (see Section 7.1). Non-uniqueness of the LSF can result in convergence problems (Allaire et al. 2004). Several of the techniques below are able to regularize the LSF and establish uniqueness.

Well-posedness of the optimization problem The optimal design of a continuum optimization problem may possess infinitely small geometrical features. In practice, this is restricted by the discretization, i.e., smaller details emerge as the discretization is refined, leading to strongly mesh-dependent solutions to the optimization problem (Bendsøe and Sigmund 2003). Well-posedness can be obtained by restricting the amount of geometrical detail using regularization and choosing an appropriate design parameterization.

Suppressing numerical artifacts and local minima Another reason to employ regularization are numerical artifacts due to insufficiencies in the finite element discretization, e.g., over-predicting local stiffness for particular element shape or material layouts. Density-based LSMs can lead to the same artifacts as are encountered in density-based TO methods. Gray areas can be represented by many small islands of material or the use of an approximate Heaviside. Also one-node connections of the material domain are possible (Van Dijk et al. 2012). A wide variety of regularization techniques is available to eliminate or reduce the appearance of numerical artifacts in the final results of a level-set-based TO.

Geometry control The final results of level-set-based TO methods may be unpractical from an engineering point of view. Often a designer wants to control certain geometrical properties, such as the smoothness of boundaries, the topological complexity and the length-scale using regularization (Chen et al. 2008; Yamada et al. 2010).

As outlined in Fig. 2 of the introduction, we distinguish between different types of regularization techniques, depending on where in the optimization procedure they are applied: LSF regularization (Section 6.1), regularization of the geometry mapping (Section 6.2) and sensitivity regularization (Section 6.3). Also the choice of design parameterization may have the effect of regularization (Section 6.4).

6.1 LSF regularization

In this subsection we discuss the most common regularization techniques in LSMs that operate directly on the LSF.

Signed-distance function regularization The convergence of an LSM can deteriorate when the magnitude of the spatial gradient of the LSF strongly varies along the zero-level contour (Sethian 1999; Osher and Fedkiw 2003; Allaire et al. 2004). To avoid this problem and establish uniqueness of the LSF for a given design, many LSMs maintain the LSF as a signed-distance function ($\|\nabla\phi\| = 1$ everywhere) (Wang et al. 2003; Allaire et al. 2004; Chen et al. 2008; Wang and Wang 2004b; Yulin and Xiaoming 2004a; Zhuang et al. 2007; Zhou and Li 2008; Challis and Guest 2009; Yamasaki et al. 2010a).

To reinitialize an LSF while approximately preserving the zero-level contour, the following PDE can be solved (Sethian 1999; Osher and Fedkiw 2003),

$$\frac{\partial\phi}{\partial\tau} + \text{sign}(\phi_0)(\nabla\phi - 1) = 0 \tag{39}$$

$$\phi_0(\boldsymbol{X}) = \phi(\boldsymbol{X}, \tau = 0). \tag{40}$$

To stabilize the numerical solution of this convective equation, upwinding schemes are most often used (Wang et al. 2003; Allaire et al. 2004; Wang and Wang 2004b; Chen et al. 2008; Challis and Guest 2009). Alternatively, Xing et al. (2010) solve the reinitialization equation by the FEM adding diffusion to stabilize the numerical results. The signed-distance function can also be explicitly recalculated (Abe et al. 2007; Yamasaki et al. 2010a).

A signed-distance reinitialization procedure usually slightly moves (smooths) the zero-level contour of the LSF (Osher and Fedkiw 2003; Hartmann et al. 2010). This typically causes inconsistencies in the optimization process (see Section 7.1). It is not possible, in general, to retain the exact location of the *discretized* contour for curved boundaries and have $\|\nabla\phi\| = 1$ everywhere. Hartmann et al. (2010) propose constrained reinitialization procedures solving the least-squares solution to the signed-distance function while keeping the location of the zero-level contour of the LSF constant.

When the LSF is maintained as a signed-distance function, holes in the interior of the material domain cannot emerge. To allow the nucleation of holes using topological gradient information, e.g., Challis and Guest (2009) and Challis (2010) only periodically reinitialize the LSF. Alternatively, holes can also be inserted in a separate step of the optimization process (see Section 4.4) (Allaire et al. 2005; Fulmański et al. 2007, 2008).

Perimeter regularization Perimeter regularization was introduced for density-based methods by Haber et al. (1996) and Petersson (1999) to obtain a well-posed optimization problem and convergent solutions with respect to mesh refinement. In level-set-based TO, many approaches also use perimeter regularization for well-posedness of the optimization problem, avoiding numerical artifacts and

smoothing of the LSF. Moreover, it also serves as stabilization of the convective HJ equation (see Section 5.1). Perimeter regularization is closely related to mean curvature flow of the LSF (Allaire et al. 2004).

The perimeter of the material domain Ω is defined as,

$$P(\Omega) = \int_{\Gamma} dS. \tag{41}$$

Maute et al. (2011) add a perimeter constraint to the optimization problem. However, a perimeter constraint may impose heavy restrictions on the potential designs and cause the optimization process to converge to sub-optimal local minima. Furthermore, the perimeter is usually not of real interest as a design requirement. Therefore, perimeter constraints should rather be incorporated in the optimization problem using a penalty formulation. The selection of an appropriate penalty factor is problem dependent (Van Dijk et al. 2012).

Maute et al. (2011) evaluate the perimeter on the aligned sub-domains of an X-FEM approach. Similarly, Van Dijk et al. (2012) compute the exact perimeter and its discrete derivative with respect to the nodal values of the LSF using a parameterization of the zero-level contour of the LSF. Yamasaki et al. (2010b) approximates the perimeter by an integral of the form of (10) in combination with an approximate Dirac function $\tilde{\delta}(\phi)$ and derives the corresponding sensitivities. All of these regularization techniques control the actual perimeter and only smooth the zero-level contour of the LSF, not promoting a flat LSF.

Instead of computing (an approximation of) the perimeter and deriving its sensitivities, perimeter penalization can be included when solving the HJ equation (see Section 5.1) using a naturally extended velocity field (see Section 4.1) (Allaire et al. 2004; Wang and Wang 2005). The shape derivative of the perimeter $P(\Omega)$ is given by the following expression (Allaire et al. 2004),

$$\delta P = \int_{\Gamma} \nabla \cdot \boldsymbol{n}\, \delta\Omega_n dS, \tag{42}$$

where $\nabla \cdot \boldsymbol{n}$ is the mean curvature of the boundary. The naturally extended velocity field based on (the negative of) (42), i.e., the mean curvature, can be written in terms of the LSF (see (27)) as,

$$v_n = \nabla \cdot \left(\frac{\nabla\phi}{\|\nabla\phi\|} \right). \tag{43}$$

Mean curvature flow is used by e.g., Allaire et al. (2004), Wang and Wang (2004b), Yulin and Xiaoming (2004a), Chen et al. (2008), Luo et al. (2008a), Zhu et al. (2010), Shojaee and Mohammadian (2011) and Mohamadian and Shojaee (2012). Often mean curvature flow is included for easier numerical treatment of the HJ equation (see also Section 5.1) and smoothing of the LSF (Wang and Wang 2005; Luo et al. 2008a). It is a form of nonlinear and anisotropic diffusion, promoting a minimal perimeter. Therefore, it also smooths the zero-level contour, but does not (necessarily) lead to a flat LSF. Perimeter penalization in this form does not only affect the perimeter but smooths the entire LSF.

Tikhonov regularization As an alternative to perimeter regularization, Tikhonov regularization (Tikhonov et al. 1995; Burger 2003), i.e. penalization of the gradient of the LSF $\|\nabla\phi\|$, is often introduced in the optimization process for the same reasons as stated above (Wang and Wang 2005; Yamada et al. 2010). In its most general form, an energy associated with the gradient of the LSF can be defined as,

$$\Pi_{\text{diff}} \sim \int_{\text{D}} \tfrac{1}{2} \nabla\phi^T\, \mathbf{C} \nabla\phi\, dV, \tag{44}$$

where $\mathbf{C}$ is a positive definite (diffusion) tensor.

For a broad range of optimization and inverse problems, energy terms such as (44) are frequently introduced via a penalty term in the formulation of the objective function for regularization purposes. Also in phase-field methods it is used, where it corresponds to the interface energy (Yamada et al. 2010) and similar approaches are common in fluid mechanics (Haber 2004).

Using integration by parts and assuming homogeneous Neumann boundary conditions for the LSF on the boundary of the *design* domain ($\partial\phi/\partial n = 0$), the derivative of (44) with respect to the LSF results in a diffusive term,

$$\delta\Pi_{\text{diff}} = \int_{\text{D}} -\nabla \cdot (\mathbf{C}\nabla\phi)\ \delta\phi\, dV. \tag{45}$$

In particular, when $\mathbf{C}$ is replaced with a scalar diffusion coefficient c_{iso}, the shape gradient of (44) takes the form of isotropic diffusion $-c_{\text{iso}}\nabla^2\phi$ (Gurtin 1996).

This type of approach has been employed by Burger (2003), Haber (2004), Liu et al. (2005), Liu and Korvink (2008), Yamada et al. (2010), Lim et al. (2011) and Otomori et al. (2011). Also, Park and Youn (2008) use diffusion to smooth the LSF in a separate step of the optimization process.

Liu et al. (2005) and Liu and Korvink (2008) introduce diffusion explicitly in their FEMLAB implementation of the LSM to add artificial dissipation for stabilizing the HJ equation. Isotropic diffusion smooths the LSF, but can also lead to a flat LSF, which in turn affects the convergence behavior of the optimization process (see Section 7.1).

Penalization of intermediate LSF values Similar to penalization of intermediate densities in density-based TO methods, distinct values of the LSF (e.g., $\phi = -c$ or $\phi = c$) can be promoted in level-set-based TO methods using penalization (Luo et al. 2009a; Wei and Wang 2009;

Mohamadian and Shojaee 2012). This type of approach is commonly used in LSMs derived from image segmentation techniques and phase-field methods (Burger and Osher 2005) and is useful to avoid flatness of the LSF near the zero-level contour. Such penalization can introduced into the generalized HJ -equation (Olsson et al. 2007) and is used e.g., in COMSOL for advancing moving interfaces using a LSF (COMSOL 2011).

Luo et al. (2009a), Wei and Wang (2009) and Mohamadian and Shojaee (2012) propose an additional constraint or penalty to the optimization process to maintain a piecewise-constant (or binary) LSF. This piecewise-constant LSF constraint or penalty causes the LSF to converge to certain plateaus and reduces the size of the region where the LSF has intermediate values usually associated with intermediate phases/density.

Penalization of intermediate LSF values may lead to a large gradient of the LSF near the zero-level contour. To mitigate this effect, it is often used in conjunction with diffusion; both techniques together determine the slope of the LSF near the zero-level contour/size of the region with intermediate density (Burger and Osher 2005). However, the strength of the penalization of intermediate LSF values and the appropriate level of diffusion needed is problem-dependent and can be difficult to determine.

6.2 Regularization of the geometry mapping

For density-based LSMs, the relation between the LSF and the material domain may be adapted to regularize the optimization problem. The boundary of the material domain can be blurred to eliminate numerical artifacts, obtain a well-posed optimization problem and obtain a smooth structural displacement field. This approach may also discourage large regions with intermediate densities and improve the convergence behavior of the optimization process.

Blurring the boundary The boundaries of the material domain in density-based LSMs involve intermediate densities, even when an exact Heaviside formulation is used (see Section 3.3). The use of an approximate Heaviside function increases the size of the region over which the boundaries is blurred depending on its bandwidth. The blurred boundary description spatially smooths the structural responses and, thus, the sensitivities (Luo et al. 2008c). This can significantly improve the convergence of the optimization process, at the cost of the crispness of the level-set-based geometry description.

Luo et al. (2008c) and Van Dijk et al. (2012) obtain the same effect using a density filter in their density-based LSMs. Using a blurred boundary, hinge connections and checkerboard patterns are avoided in the density-based description of the material domain. Norato et al. (2004) use a filtering technique in the geometry mapping to avoid issues with non-differentiability of the volume fraction for certain configurations of the design parameterization.

Density penalization Similar to density-based TO methods, penalization of intermediate densities can be employed in density-based LSMs to avoid large regions with intermediate densities (Guo et al. 2005; Kawamoto et al. 2011; Van Dijk et al. 2012). However, in most LSMs large areas of intermediate density are eliminated by other types of regularization (e.g., signed distance reinitialization) rather than using density penalization. When densities are used as intermediate variables, in principle all regularization techniques that have been proposed for density-based TO methods can also be adopted in a level-set-based TO method.

6.3 Sensitivity regularization

In density-based TO methods, sensitivity filtering was proposed by Sigmund (1994) to avoid mesh-dependent solutions. Similarly, sensitivity information can be altered in level-set-based TO methods to obtain smooth designs and reduce the likelihood to converge prematurely to local minima. Velocity extensions, extra- and interpolation of velocity fields have a smoothing effect. Explicit filtering techniques, including spatial filters and point-wise mappings/scaling of sensitivities, may be employed to further smooth the sensitivity field.

Velocity extension The application of velocity extensions, such as the Helmholtz (Yamasaki et al. 2011) and the Hilbertian (De Gournay 2006) extension, has a regularizing effect on the velocity. Velocity extensions can conserve consistency of the sensitivity field when the design velocity on the boundary of the material domain is preserved with respect to the particular scalar product (needed for calculation of Lagrange multipliers of constraints) that is used in the optimization process.

Sensitivity extrapolation Allaire et al. (2004) evaluate the velocity at the center of finite elements and extrapolate it to the nodes of finite elements (personal communication). Also Amstutz and Andrä (2006) and Ha and Cho (2008a) use extrapolation of the sensitivity values. In the work of Abe et al. (2007) and Ha and Cho (2008a, b) a conforming mesh is used for the structural analysis. The sensitivity information calculated on this mesh is redistributed to the fixed regular grid of the LSF.

Sensitivity smoothing Explicit smoothing procedures of the design velocity are often employed in level-set-based TO methods that are based on variational shape-sensitivity

analysis (Wang and Wang 2004b, 2006b; Wang et al. 2007a; Challis and Guest 2009; Challis 2010; Yamasaki et al. 2011). For instance, Challis and Guest (2009) and Challis (2010) use a spatial filtering technique to smooth the sensitivity fields before the design update.

Sensitivity scaling and clipping Alternatively, a local scaling of the velocity field, also called nonlinear velocity mapping, e.g., $v_n(\boldsymbol{X}) = \arctan(v_n(\boldsymbol{X}))$, is used to soften peak sensitivities and enhance the regularity of the sensitivity field (Wang et al. 2004; Yulin and Xiaoming 2004a; Rong and Liang 2008). For example, Yulin and Xiaoming (2004a) and Rong and Liang (2008) use a nonlinear velocity mapping and maintain the orthogonality of the steepest-descent direction with the gradient of active constraints. Liu et al. (2005) cut off peak values of the sensitivity of a compliance response function to improve the convergence behavior.

Regularized sensitivity fields can improve the convergence behavior of the optimization process, help avoiding numerical artifacts and local minima and lead to smooth boundaries. However, altering of sensitivities often leads to numerically inconsistent sensitivities which may affect the convergence, in particular close to an optimum (see Section 7.1). When altering the sensitivities, one needs to ensure that the update procedure indeed improves the design.

6.4 LSF parameterization

The resolution of the LSF parameterization has a direct effect on the design resolution and feature size (Luo et al. 2007; Norato et al. 2007; Frei et al. 2008). The LSF parameterization can also be chosen such that small features, checkerboard patterns and/or areas of intermediate densities are suppressed (Van Dijk et al. 2012).

A parameterization may be chosen such that large variations of the gradient of the LSF on the boundary are less likely, improving the convergence behavior of the optimization process (see Section 7.1). For example, this is accomplished by Pingen et al. (2010) and Kreissl et al. (2011) using an approximate maximum formulation for the parameterization of the LSF (see Section 2.4).

To avoid non-smooth boundaries and limit the amount of spatial variations of the LSF it is also possible to apply filtering schemes. Abe et al. (2007) and Maute et al. (2011) use a filtering scheme to smooth the LSF. Kawamoto et al. (2011) use a filtering technique based on the Helmholtz equation to smoothen the LSF. For density-based TO the same filtering technique is used e.g., by Lazarov and Sigmund (2011). To avoid inconsistencies in the optimization process, the filtering scheme should be taken into account in the derivation of the sensitivity information.

In general it may be beneficial to choose a parameterization of the LSF independent of the discretization of the structural model and such that the optimization problem can be solved most efficiently. Also designs can be come overly smooth when the design freedom is restricted too much, as Luo et al. (2007) have shown in a study comparing different support sizes of RBFs.

7 Discussion

The application of the LSM to TO allows for a clear and crisp definition of the material domain. Depending on the geometry mapping the crispness is either retained in the mechanical model, using IBTs or conforming meshes, or blurred along the material boundary, using density-based approaches. Mesh-independent results with smooth boundaries have been demonstrated as a result of heavy use of regularization techniques. Most LSMs should be interpreted as shape optimization methods with the potential to change the topological complexity.

In comparison to density-based TO, LSMs often suffer from a poor rate of convergence and require a large number of iterations in the optimization process. As discussed below, to improve the convergence behavior and to obtain satisfactory results, it is important to control the slope and smoothness of the LSF both near the boundary and within the design domain.

Subsequently, we elaborate on the main aspects that influence the convergence rate of an LSM (Section 7.1), different means to control the LSF and resulting designs (Section 7.2) and the nucleation of holes in an LSM (Section 7.3). Furthermore, we discuss the similarities between, in particular, density-based LSMs and other TO methods (Section 7.4).

7.1 Convergence rate of an LSM

The convergence rate of an LSM depends on the choices for its different components discussed earlier: the LSF parameterization, the geometry mapping, the formulation of the optimization problem, the update information, the update procedure and the regularization. Key issues for the convergence rate are the convexity and the nonlinearity of the optimization problem and the choice of sensitivity analysis and regularization techniques.

Convexity and nonlinearity The convexity of the optimization problem directly determines the level of difficulty of solving it, manifests itself in the existence or absence of local minima and depends on the formulation of objective, constraints, and design parameters of the optimization

problem at hand. For instance, compliance minimization problems are usually easy to solve and compliant mechanism design problems more difficult. It is important to realize that the choice of design parameterization (i.e., the optimization variables) has an influence on the convexity of the optimization problem. If possible, it should be chosen to preserve or increase the convexity.

In addition to convexity, a large degree of nonlinearity of the optimization problem can complicate finding the solution of a particular optimization problem. Not only the LSF parameterization, but also the geometry mapping and the discretization of the structural model influence the degree of nonlinearity of the optimization problem.

The degree of nonlinearity between variations of the LSF and changes of the geometry depends on the magnitude of spatial gradient of the LSF along the material boundaries (Pingen et al. 2010; Van Dijk et al. 2012). For a given variation of the LSF, a steep LSF results in little boundary displacement whereas a flat LSF leads to a large boundary displacement, see Fig. 12.

This dependency is reflected in parametrized shape sensitivities (see (29)) and can lead to convergence problems in the optimization process due to two effects (Pingen et al. 2010; Van Dijk et al. 2012). Firstly, for a flat LSF the sensitivity information only provides accurate predictions of changes of the response functions for very small variations of the LSF. Secondly, strong variations of the slope of the LSF along the zero-level contour cause ill-conditioning of the optimization process. For HJ-based LSMs, the magnitude of the spatial gradient of the LSF affects the convergence rate of explicit time integration schemes where the local step size is determined as $\Delta\phi = v_n\|\nabla\phi\|\Delta\tau$ (see Section 5.1), i.e., the slope of the LSF influences the step size limited by the CFL criterion (Allaire et al. 2004). Therefore, it is preferred to have a uniform gradient of the LSF on the interface, e.g., $\|\nabla\phi\| \approx 1$. Measures to control the slope of the LSF are discussed in Section 7.2.

A high degree of nonlinearity and non-convexity can increase the likelihood that the optimization process converges to local minima. A thorough investigation into local minima arising in standard level-set-based optimization problems (even for compliance minimization) is not yet available. In LSMs without hole nucleation mechanisms the results are highly dependent on the initial configuration, which is a clear sign of nonconvexity. Seeding an initial design with a large number of holes or inclusions may lead to numerical issues and does not necessarily mitigate the dependency of the final result on the initial guess. LSMs allowing hole nucleation as well as pure density-based methods suffer less from this problem.

Adapting the LSF parameterization and adding regularization alters the design space and convexity of the optimization problem. Selecting a proper parameterization of the LSF and filtering schemes for the LSF (see Section 6.4) can improve the convergence rate of a level-set-based TO by altering the design space, and therefore, the convexity and nonlinearity. Filtering increases the radius of influence of individual optimization variables. However, care has to be taken to ensure that designs do not become overly smooth and/or lose essential topological detail.

Sensitivities and regularization The convergence rate of the optimization process depends heavily on the sensitivities and associated regularization techniques. An important aspect is the consistency of the optimization process.

Numerically consistent sensitivities can be obtained by differentiation of the discretized responses with respect to the optimization variables (Van Keulen et al. 2005), see Fig. 13. Alternatively, variational or continuum sensitivities are obtained by differentiation the continuum version of the structural model. Discretizing response functions and their variational sensitivities may lead to a discrepancy between the discretized variational sensitivities and the exact derivatives of the discretized system, i.e., inconsistencies (Van

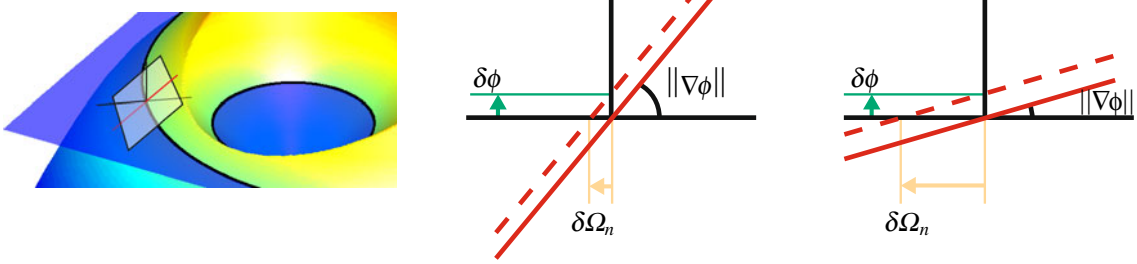

(a) Tangent plane to the LSF on the interface for a two-dimensional domain.

(b) Small boundary displacement due to a steep LSF.

(c) Large boundary displacement due to a flat LSF.

Fig. 12 A boundary variation due to a variation of the LSF depends on the spatial gradient of the LSF on the interface

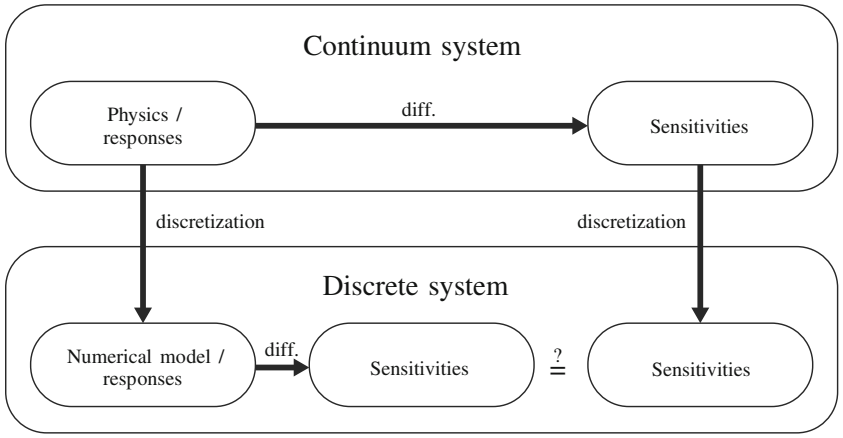

Fig. 13 Consistency of sensitivities

Keulen et al. 2005). The consistency of sensitivities can be validated using rigorous finite difference testing.

Sources of inconsistencies can be (a) variational sensitivities (shape sensitivities or topological derivatives), (b) approximations involved in the evaluation of the sensitivity information, (c) interpolation/extrapolation of sensitivity fields and (d) regularization techniques. For instance, adding diffusion, signed-distance reinitialization (see Section 6.1) and sensitivity smoothing (see Section 6.3) introduce inconsistencies when these are not accounted for in the sensitivity analysis.

Numerically consistent sensitivities accurately predict the behavior of the applied numerical model for small design changes, yet they do not necessarily lead to the best search direction. This depends on the problem at hand and on whether the goal of the optimization is to find the solution to the discretized problem or the underlying continuum problem (Sigmund and Maute 2012). Consistency is essential when one is interested in finding a Karush–Kuhn–Tucker (KKT) point of the discretized optimization problem. It is also important for studying and understanding the fundamental difficulties of solving a particular optimization problem. It can be crucial for the treatment of multiple constraints to accurately describe the constraint surface and avoid oscillations in the optimization process. Moreover, it is preferred to start from a consistent framework when adding inconsistencies for regularization purposes (Van Dijk et al. 2012).

On the other hand, numerical artifacts and convergence to local minima with poor performance can be avoided by the usage of inconsistent sensitivity information (Sigmund 1994). Solutions to level-set-based TO problems are dependent on the initial design and converging to a local minimum is general issue (Van Dijk et al. 2012). Guided by regularized but inconsistent sensitivity information, the optimization process may avoid converging to a local minimum with poor performance. The mesh dependency of the optimization results can be mitigated by sensitivity smoothing (see Section 6.3) and diffusion of the LSF (see Section 6.1).

7.2 Control of the LSF

Controlling the slope and the smoothness of the LSF are important for the convergence behavior of the optimization process and the shape of the final designs.

Controlling the slope The slope of the level-set function $\|\nabla\phi\|$ on the interface is not only important for the convergence rate of the optimization process (see Section 7.1), but, in case of density-based LSMs, also for the crispness of the material interface (i.e., amount of elements with intermediate densities). For density-based LSMs using an approximate Heaviside function, even elements that are not intersected by the material interface may have intermediate densities (see Section 3.3). For these methods a flat LSF near the zero-level contour leads to large areas of intermediate density. To obtain a constant width of the blurred interface, a uniform gradient of the LSF is required along the boundary of the design.

To control the slope of the LSF, different regularization techniques are popular in level-set-based TO methods (see Section 6.1). A reinitialization procedure is often used to maintain the LSF as a signed-distance function, ensuring $\|\nabla\phi\| = 1$ (e.g., Wang et al. 2003; Allaire et al. 2004). Introducing diffusion into the LSF (e.g., Liu and Korvink 2008) reduces the magnitude of the gradient of the LSF and penalization of intermediate LSF values (e.g., Mohamadian and Shojaee 2012) can avoid the occurrence of areas with a flat LSF near the zero-level contour.

The LSF parameterization can be chosen such that excessive differences of the gradient of the LSF along the interface are avoided. The usage of parametrized geometric shapes has the potential to produce spatial gradients of the

LSF of equal magnitude (see Section 2.4). Also introducing bounds for the LSF can limit the non-uniformity of the gradient of the LSF.

Control of the smoothness The smoothness of the LSF and, in particular, of its zero-level contour determines the level of geometrical detail and smoothness of the boundaries of the final design. Controlling the smoothness can also prevent numerical artifacts, reduce mesh dependency of solutions (see Section 6) and/or stabilize solving the HJ equation (see Section 5.1).

The smoothness of the LSF is often increased using different kinds of diffusion (see Section 6.1). The appropriate strength of smoothing the LSF is problem dependent. Introducing too much smoothing can cause overly smooth designs and the loss of important details of a design.

In general, the exact influence that regularization has on the resulting designs is not known a priori. Therefore, the designer does not have full control over the effect that regularization has on the geometry of the final designs. Moreover, when regularization methods are introduced into the formulation of the design problem, it may become unclear what optimization problem is solved.

7.3 Hole nucleation

The ability for LSMs to nucleate holes in the interior of the material domain can be accomplished using topological derivatives and, to a lesser degree, using a natural velocity extension or an approximate-Heaviside-based density formulation.

Topological derivative Topological derivatives can be used to insert holes in a separate step of the optimization process (see Section 4.4). In this manner, altering topological complexity is the result of sensitivity information. However, whenever a new hole is inserted, essentially a new optimization problem is generated. To avoid convergence problems the frequency with which a hole is inserted needs to be chosen carefully.

Alternatively, topological derivatives are introduced as a reaction term in the HJ equation (see Section 5.1). While this approach leads to a more elegant procedure, introducing a finite sized hole also leads to discrete and non-differentiable step in the optimization process, potentially affecting the converge rate (see Section 7.1).

Natural velocity extension HJ-based LSMs are also able to generate holes when using a natural velocity extension (see Section 7.4). Even though this nucleation is incidental, it often leads to an improvement performance due to the similarity between naturally extended velocity fields and density sensitivities (see Section 7.4). Again, introducing a finite sized hole may affect the converge of the optimization process.

Approximate Heaviside Density-based LSMs that are based on an approximate Heaviside formulation can also generate new holes along the structural boundary as locally the method resembles a density-based TO method.

7.4 Relation to other TO methods

In the literature, density-based and level-set-based TO methods are often treated as fundamentally different approaches. However, both types of methods share several commonalities, and also phase field approaches for TO have strong similarities with level-set-based TO methods (Burger and Osher 2005; Zhou and Wang 2007). For a more detailed explanation of the relation between phase-field methods and LSMs we refer to the survey of LSMs by Burger and Osher (2005). In this section we point out some similarities between *density-based* LSMs, density-based TO methods and phase-field methods, focusing on the geometry mapping, update information, update procedure and regularization.

Geometry mapping Mechanical models based on a density distribution are used in density-based TO methods, density-based LSMs and phase-field methods. The main difference concerns the parameterization of the density distribution. In density-based TO and phase-field methods the parameters controlling the density distribution are directly treated as the optimization variables, whereas in level-set-based TO methods the optimization variables define the parameters of a discretized LSF and the density distribution is used as an intermediate field in the mechanical model.

Density-based LSMs map the LSF into a density distribution using an exact or approximate Heaviside function. Using an exact Heaviside formulation, only elements that are intersected by the zero-level contour of the LSF are assigned intermediate density values. This type of approach can still create similar numerical artifacts as density-based TO methods in the absence of regularization techniques (Van Dijk et al. 2012).

For an approximate Heaviside formulation, all densities within the smeared interface layer ($-h \leq \phi \leq h$) can be altered and, therefore, the level-set-based optimization locally behaves as a density-based TO method. Without regularization this may lead to large areas of intermediate densities $\varepsilon < \rho_e < 1$. Methods that directly map an LSF value into an element density (see Section 3.3) can be regarded as a type of density-based TO approach. The optimization variables $-\infty \leq s_i \leq \infty$ (i.e., nodal values of the LSF) are directly mapped into density variables $\varepsilon \leq \rho_e \leq 1$, where the side bounds of the densities

are incorporated through the approximate Heaviside formulation. In this regard, LSMs directly mapping the LSF into a density distribution via an approximate Heaviside function share great commonality with and blur the difference between density-based TO using projection schemes, e.g., Guest (2009b), Kawamoto et al. (2011), Lazarov and Sigmund (2011) and Wang et al. (2011).

Usually, density-based LSMs use a relatively small bandwidth (in the order of the finite-element spacing). However, large or even infinitely large bandwidths (e.g., using an arctangent function (Haber 2004; Gomes and Suleman 2006)) can be used, leading to similar behavior as density-based TO methods.

For density-based LSMs (in particular using an approximate Heaviside function), the presence of (intermediate) densities allows for changing the topology in the same way as density-based TO methods. The drawback is that all potential problems of density-based TO are also inherited. Therefore, regularization approaches are used to retain the shape-optimization character of LSMs.

Update information There are strong similarities between naturally extended velocity fields, topological derivatives and density sensitivities. For illustration purposes, we study the expressions for the compliance of a structure, assuming a linear elastic response and neglecting body forces and design-dependent loads.

Naturally extended velocity field A naturally extended normal velocity field is based on the variational shape gradient $\mathrm{d}_{\mathcal{S}}R$. Using the same notation as before, the shape gradient $\mathrm{d}_{\mathcal{S}}R$ on the homogeneous Neumann boundary corresponding to the compliance is given by,

$$\mathrm{d}_{\mathcal{S}}R = -\boldsymbol{\epsilon}(\boldsymbol{u}) : \mathbf{C} : \boldsymbol{\epsilon}(\boldsymbol{u}), \tag{46}$$

which is the negative of the local strain energy density (Allaire et al. 2004, Eq. 24).

Van Dijk et al. (2010) directly discretize (46) as,

$$\mathrm{d}_{\mathcal{S}}R^e = -\boldsymbol{u}_e{}^T \mathbf{K}_e \boldsymbol{u}_e, \tag{47}$$

where the scalar $\mathrm{d}_{\mathcal{S}}R^e$ is the per-element value of the shape gradient, $\mathbf{K}_e$ is the original element stiffness matrix of a (full material) element and $\boldsymbol{u}_e$ is the discrete element displacement vector.

Alternatively, one can represent the stiffness of an intersected element via an effective stiffness tensor (or Young's modulus) which a function of the geometry $\mathbf{C} = \mathbf{C}(\Omega)$ and, therefore, of the density ρ_e. Allaire et al. (2004) discretize the per-element shape gradient $\mathrm{d}_{\mathcal{S}}R^e$ as,

$$\mathrm{d}_{\mathcal{S}}R^e = -\boldsymbol{u}_e{}^T (\rho_e \mathbf{K}_e)\, \boldsymbol{u}_e. \tag{48}$$

The element-wise shape gradient $\mathrm{d}_{\mathcal{S}}R^e$ is then extrapolated to the nodes of finite elements (personal communication). These two choices of the representation of the naturally extended normal velocity field lead to different optimization results. Often, the precise implementation of the velocity fields is unfortunately omitted and it remains unclear what formulation is used.

Density derivative Alternatively, the same density-based mechanical model can be used in density-based TO methods, scaling the element stiffness with penalized element density ρ_e^p, where p is the penalization exponent (Bendsøe 1989; Zhou and Rozvany 1991). Density-based TO methods use the discrete derivatives of the compliance with respect to the densities ρ_e,

$$\frac{\partial R}{\partial \rho_e} = -\boldsymbol{u}_e{}^T \left(p\, \rho_e^{p-1} \mathbf{K}_e \right) \boldsymbol{u}_e, \tag{49}$$

to update the optimization variables. Without penalization ($p = 1$), (49) is equivalent to (47). With a penalization exponent of $p = 2$, (49) is exactly twice the value of (48). For compliance, we observe that shape-sensitivity-based velocity fields closely resemble density sensitivities depending on the choice of discretization.

Topological derivative In particular cases such as the compliance, topological derivatives are also similar to shape and density sensitivity fields as recognized earlier by Guo et al. (2005). Expressions for the topological derivative of a response function have previously been derived from shape sensitivity analysis (Céa et al. 2000; Novotny et al. 2003; Burger et al. 2004; He et al. 2007). Note that the topological derivative has the opposite sign of the corresponding shape derivative, because it concerns the removal of material.

However, more commonly expressions for the topological derivative are derived from asymptotic expansion of the objective functional (Garreau et al. 2001; Sokołowski and Żochowski 2001). Also these expressions have similarities with the shape derivative, e.g., for compliance they are a combination of the strain energy density and the traces of the strain and stress tensors.

For clarity and reproducibility of the results, authors should discuss the discretization of sensitivity fields. In this review paper we have identified strong similarities between naturally extended velocity fields, topological derivatives and density sensitivities of the compliance. For an arbitrary response function this does not need to be the case. Further investigations on this subject are needed to shed light on the interdependence of the different types of sensitivity information for different types of response functions.

Update procedure Originally, the HJ equation was used to update the LSF (see Section 5.1). This approach is

fundamentally different from density-based methods as it restricts geometry changes to the vicinity of the material boundary. HJ-based LSMs that only use a reaction term in the HJ equation (defined everywhere in the design domain, e.g., Yamada et al. 2010) are again close to using a density-based TO method. The majority of density-based methods employ mature and efficient mathematical programming algorithms. Recently, these algorithms have also been adopted in level-set-based TO methods.

Regularization The regularization techniques used in LSMs are related to those used in density-based TO methods and phase field approaches. Originally density-based LSMs employed signed-distance reinitialization techniques to maintain the regularity of the LSF (see Section 6.1). Consistent filtering techniques (e.g., Luo et al. 2008c) and penalization of intermediate densities (e.g., Guo et al. 2005) used in density-based TO methods have also been applied to LSMs to control the geometry of the final result. Furthermore, regularization techniques originally developed for the interfacial dynamics in phase field methods have also been adopted in LSMs (Zhu et al. 2010; Mohamadian and Shojaee 2012) to obtain a finite width of the interface layer (Burger and Osher 2005).

To mitigate the mesh-dependency in density-based methods the perimeter is approximated via the norm of the spatial gradients of the density distribution and penalized (Haber et al. 1996). The same approach has been applied in LSM penalizing the gradients of the LSF. The concepts of interfacial energy (e.g., Yamada et al. 2010) and piecewise constant functions (e.g., Mohamadian and Shojaee 2012) have been derived from phase field approaches. The same filtering techniques can be used for level-set and density fields such as the Helmholtz filter (Kawamoto et al. 2011; Lazarov and Sigmund 2011).

Density-based methods, LSMs and phase-field methods employ (combinations of) the same or similar regularization techniques and their classification can be ambiguous. For instance, both Takezawa et al. (2010) and Choi et al. (2011) employ independently the same regularization for density-based TO as Yamada et al. (2010) for level-set-based TO.

Independent of whether the primary optimization variables define a density distribution, a LSF, or an auxiliary field, the functional relationships between the physical properties in the mechanical model and the optimization variables may be rather similar. Therefore, the boundaries between density-based TO methods and LSMs are vanishing. The remaining difference between density-based TO and the LSMs is the update procedure, where most LSMs restrict the geometry changes to the vicinity of material boundary and density-based TO alter the design in the entire design domain. Introducing Heaviside-type projection schemes into density-based TO and enhancing LSMs with hole nucleation features further blurs the difference between TO approaches.

8 Conclusions and recommendations

The goal of this review paper was to provide an overview of level-set-based TO in the past decade, as well as to categorize the various approaches and highlight their relations and interdependence. Here, we summarize the most important features and challenges of LSMs, and conclude with recommendations for future research.

The application of the LSM for TO allows for a clear and crisp definition of the geometry by iso-contours of the LSF. To retain this crispness in the mechanical model an appropriate type of geometry mapping needs to be used, i.e., IBTs or conforming discretization. Density-based level-set methods blur the boundary to a certain extent, where the amount of intermediate densities in the mechanical model depends on the type of Heaviside function (exact or approximate and the size of the bandwidth). A crisp description of the boundary is essential for the application of TO to problems where the accuracy of the structural response along the interface is important. LSMs are also a promising alternative to density-based TO when the optimization process has a strong tendency to lead to intermediate states or when intermediate states lead to convergence problems in the structural analysis.

Most types of LSMs can be interpreted as a generalized form of shape optimization with the potential to change the topological complexity. Using an LSM, the parameterization of the shape of a design is straight-forward and allows for topological changes. To enhance the topology of designs, mechanisms for hole nucleation may be added to LSMs using topological derivatives or natural extended velocity fields (resembling the sensitivity fields of density-based TO methods). Density-based LSMs that use an approximate Heaviside formulation locally behave like density-based TO methods where the LSF is within the bandwidth of the approximate Heaviside. This property may also be employed to generate new holes, but comes at the cost of loss of crispness of the mechanical model.

Challenges Level-set-based TO methods suffer from local minima and dependency of the final result on the initial guess. This property is a consequence of the shape optimization character of LSMs. Seeding an initial design with a large number of holes or inclusions may lead to numerical issues and does not necessarily mitigate the dependency of the final result on the initial guess.

The results of level-set-based TO methods rely heavily on regularization techniques. To suppress numerical artifacts in density-based LSMs, regularization techniques such as

sensitivity smoothing, diffusion and signed-distance reinitialization need to be applied. Furthermore, regularization is needed to improve the convergence of the optimization process. Regularization is also often employed to avoid convergence to local minima with poor performance.

The construction of sensitivity fields, the type of update procedure and the application of regularization can result in inconsistencies in the optimization process. Numerical consistency does not necessarily lead to fast convergence. However, consistency is essential to find a KKT point of the discretized optimization problem. Furthermore, it is important for understanding the mathematical properties of a particular optimization problem, the potential of a proposed approach and its fundamental problems. Inconsistencies may be introduced in a later stage for specific purposes, such as regularization, and in a controlled manner.

The treatment of constraints can be difficult in a steepest-descent type LSMs, in particular the ones based on the HJ equation. A shift of LSMs towards mathematical programming methods is observed to solve optimization problems more efficiently and avoid oscillations. This approach often introduces regularization into the formulation of the optimization problems while HJ-based update procedures typically include regularization techniques implicitly.

One of the main challenges of level-set-based TO is the convergence behavior, apparent by oscillations in the optimization process and/or slow design evolution. The convergence is typically improved by controlling the slope and the smoothness of the LSF along the material boundary. Control of the LSF can be obtained using regularization techniques and a smart choice of LSF parameterization.

Recommendations To retain the crispness of a level-set-based design interpolation, a crisp geometry mapping needs to be used. The majority of level-set-based topology optimization methods are still based on a density field. In this respect, methods using conforming discretization or IBTs (e.g., X-FEM) are promising for the treatment of design-dependent (boundary) loads and other boundary phenomena that should be captured in the numerical modeling.

Future research on LSMs should devote particular attention to clearly identifying and systematically analyzing the influence of the different components of LSMs. This is in particular important when the update procedures include regularization, and for more involved geometry mappings and LSF parameterizations. The convergence behavior and numerical cost of LSMs should be clearly analyzed with well established benchmark problems, isolating different contributing factors.

Owing to the complexity of LSMs, we recommend to clearly present all components LSMs or refer to appropriate references where the components are described in sufficient detail. This includes the LSF parameterization, geometry mapping, structural model, update information, update procedure, and regularization techniques. For the LSM research community, it is of crucial importance to compare the different formulations and numerical techniques used in these components to other LSMs as well as to density-based and phase field TO methods. All information needs to be presented in sufficient detail to allow other researchers to reproduce the optimization methods and results. We encourage researchers in the field to provide access to the codes used to generate the published results.[2]

As this overview has shown, the boundaries between level-set and density-based topology optimization methods have blurred in the past decade. We feel that developing a unified understanding that encompasses all TO approaches will enhance future research and progress in TO. In particular for density-based LSMs, the relations to techniques used in density-based TO and phase-field methods need to be clearly identified and the performance compared. The field of TO should be seen as a single field of research and much can be gained by drawing parallels and exchanging techniques among the different TO approaches.

Acknowledgements The authors would like to gratefully acknowledge the support of the National Science Foundation under grant EFRI-1038305 (second author) and the Dutch MicroNed programme (other authors). The opinions and conclusions presented in this paper are those of the authors and do not necessarily reflect the views of the sponsoring organization. We are grateful for the insights Professor Grégoire Allaire, Ecole Polytechnique, France, shared with us.

References

Abe K, Kazama S, Koro K (2007) A boundary element approach for topology optimization problem using the level set method. Commun Numer Methods Eng 23(5):405–416

Allaire G, Jouve F (2005) A level-set method for vibration and multiple loads structural optimization. Comput Methods Appl Mech Eng 194(30–33):3269–3290

Allaire G, Jouve F (2008) Minimum stress optimal design with the level set method. Eng Anal Bound Elem 32(11):909–918

Allaire G, Bonnetier E, Francfort G, Jouve F (1997) Shape optimization by the homogenization method. Numer Math 76(1):27–68

Allaire G, Jouve F, Toader AM (2002) A level-set method for shape optimization. CR Math 334(12):1125–1130

Allaire G, Jouve F, Toader AM (2004) Structural optimization using sensitivity analysis and a level-set method. J Comput Phys 194(1):363–393

Allaire G, De Gournay F, Jouve F, Toader AM (2005) Structural optimization using topological and shape sensitivity via a level set method. Control Cybern 34(1):59–80

Allaire G, Dapogny C, Frey P (2011) Topology and geometry optimization of elastic structures by exact deformation of simplicial mesh. CR Math 349(17–18):999–1003

[2]Some implementations can be found on the internet: The codes of G. Allaire, V.J. Challis, N.P. van Dijk and M.Y. Wang.

Ambrosio L, Buttazzo G (1993) An optimal design problem with perimeter penalization. Calc Var Partial Differ Equ 1(1): 55–69

Amstutz S (2011) Connections between topological sensitivity analysis and material interpolation schemes in topology optimization. Struct Multidisc Optim 43(6):755–765

Amstutz S, Andrä H (2006) A new algorithm for topology optimization using a level-set method. J Comput Phys 216(2):573–588

Belytschko T, Xiao SP, Parimi C (2003) Topology optimization with implicit functions and regularization. Int J Numer Methods Eng 57(8):1177–1196

Bendsøe MP (1989) Optimal shape design as a material distribution problem. Struct Optim 1(4):193–202

Bendsøe MP, Kikuchi N (1988) Generating optimal topologies in structural design using a homogenization method. Comput Methods Appl Mech Eng 71(2):197–224

Bendsøe MP, Sigmund O (1999) Material interpolation schemes in topology optimization. Arch Appl Mech 69(9–10):635–654

Bendsøe MP, Sigmund O (2003) Topology optimization: theory, methods, and applications. Springer, Berlin

Bletzinger KU, Kimmich S, Ramm E (1991) Efficient modeling in shape optimal design. Comput Syst Eng 2(5–6):483–495

Bourdin B, Chambolle A (2003) Design-dependent loads in topology optimization. ESAIM Control Optim Calc Var 9:19–48

Brooks AN, Hughes TJR (1982) Streamline upwind/Petrov–Galerkin formulations for convection dominated flows with particular emphasis on the incompressible Navier–Stokes equations. Comput Methods Appl Mech Eng 32(1):199–259

Bruyneel M, Duysinx P, Fleury C (2002) A family of MMA approximations for structural optimization. Struct Multidisc Optim 24(4):263–276

Burger M (2003) A framework for the construction of level set methods for shape optimization and reconstruction. Interfaces Free Bound 5(3):301–330

Burger M, Osher S (2005) A survey on level set methods for inverse problems and optimal design. Eur J Appl Math 16(2):263–301

Burger M, Hackl B, Ring W (2004) Incorporating topological derivatives into level set methods. J Comput Phys 194(1): 344–362

Céa J, Garreau S, Guillaume P, Masmoudi M (2000) The shape and topological optimizations connection. Comput Methods Appl Mech Eng 188(4):713–726

Cecil T, Qian J, Osher S (2004) Numerical methods for high dimensional Hamilton–Jacobi equations using radial basis functions. J Comput Phys 196(1):327–347

Challis VJ (2010) A discrete level-set topology optimization code written in Matlab. Struct Multidisc Optim 41(3):453–464

Challis VJ, Guest JK (2009) Level set topology optimization of fluids in Stokes flow. Int J Numer Methods Eng 79(10):1284–1308

Chen S, Chen W (2011) A new level-set based approach to shape and topology optimization under geometric uncertainty. Struct Multidisc Optim 44(1):1–18

Chen S, Wang MY, Liu AQ (2008) Shape feature control in structural topology optimization. Comput-Aided Des 40(9):951–962

Chen S, Chen W, Lee S (2010) Level set based robust shape and topology optimization under random field uncertainties. Struct Multidisc Optim 41(4):507–524

Choi KK, Kim NH (2005) Structural sensitivity analysis and optimization: linear systems, vol 1. Springer, New York

Choi JS, Yamada T, Izui K, Nishiwaki S, Yoo J (2011) Topology optimization using a reaction-diffusion equation. Comput Methods Appl Mech Eng 200(29–32):2407–2420

COMSOL (2011) COMSOL multiphysics user's guide, version 4.2a

De Gournay F (2006) Velocity extension for the level-set method and multiple eigenvalues in shape optimization. SIAM J Control Optim 45(1):343–367

De Gournay F, Allaire G, Jouve F (2008) Shape and topology optimization of the robust compliance via the level set method. ESAIM Control Optim Calc Var 14(01):43–70

De Ruiter MJ, Van Keulen F (2000) Topology optimization: approaching the material distribution problem using a topological function description. In: Topping BHV (ed) Computational techniques for materials, composites and composite structures, Edinburgh, United Kingdom, pp 111–119

De Ruiter MJ, Van Keulen F (2001) Topology optimization using the topology description function approach. In: Cheng G, Gu Y, Liu S, Wang Y (eds) 4th World congress on structural and multidisciplinary optimization, Dailan, China

De Ruiter MJ, Van Keulen F (2002) The topological derivative in the topology description function approach. In: Gosling P (ed) Engineering design optimization, product and process improvement, ASMO UK/ISSMO: University of Newcastle-upon-Tyne

De Ruiter MJ, Van Keulen F (2004) Topology optimization using a topology description function. Struct Multidisc Optim 26(6):406–416

Duan XB, Ma YC, Zhang R (2008) Shape-topology optimization for Navier–Stokes problem using variational level set method. J Comput Appl Math 222(2):487–499

Eschenauer HA, Olhoff N (2001) Topology optimization of continuum structures: a review. Appl Mech Rev 54:331

Eschenauer HA, Kobelev VV, Schumacher A (1994) Bubble method for topology and shape optimization of structures. Struct Multidisc Optim 8(1):42–51

Fleury C, Braibant V (1986) Structural optimization: a new dual method using mixed variables. Int J Numer Methods Eng 23(3):409–428

Frei WR, Tortorelli DA, Johnson HT (2007) Geometry projection method for optimizing photonic nanostructures. Opt Lett 32(1):77–79

Frei WR, Johnson HT, Tortorelli DA (2008) Optimization of photonic nanostructures. Comput Methods Appl Mech Eng 197(41–42):3410–3416

Fries TP, Belytschko T (2010) The extended/generalized finite element method: an overview of the method and its applications. Int J Numer Methods Eng 84(3):253–304

Fulmański P, Laurain A, Scheid JF, Sokołowski J (2007) A level set method in shape and topology optimization for variational inequalities. Int J Appl Math Comput Sci 17(3):413–430

Fulmański P, Laurain A, Scheid JF, Sokołowski J (2008) Level set method with topological derivatives in shape optimization. Int J Comput Math 85(10):1491–1514

Garreau S, Guillaume P, Masmoudi M (2001) The topological asymptotic for PDE systems: the elasticity case. SIAM J Control Optim 39:1756

Gomes AA, Suleman A (2006) Application of spectral level set methodology in topology optimization. Struct Multidisc Optim 31(6):430–443

Groenwold AA, Etman LFP (2008) On the equivalence of optimality criterion and sequential approximate optimization methods in the classical topology layout problem. Int J Numer Methods Eng 73(3):297–316

Groenwold AA, Etman LFP (2010) A quadratic approximation for structural topology optimization. Int J Numer Methods Eng 82(4):505–524

Guest JK (2009a) Imposing maximum length scale in topology optimization. Struct Multidisc Optim 37(5):463–473

Guest JK (2009b) Topology optimization with multiple phase projection. Comput Methods Appl Mech Eng 199(1–4):123–135

Guest JK, Prévost JH, Belytschko T (2004) Achieving minimum length scale in topology optimization using nodal design variables and projection functions. Int J Numer Methods Eng 61(2): 238–254

Guo X, Zhao K, Wang MY (2005) A new approach for simultaneous shape and topology optimization based on dynamic implicit surface function. Control Cybern 34(1):255–282

Gurtin ME (1996) Generalized Ginzburg–Landau and Cahn–Hilliard equations based on a microforce balance. Phys D 92(3–4):178–192

Ha SH, Cho S (2005) Topological shape optimization of heat conduction problems using level set approach. Numer Heat Transf, B Fundam 48(1):67–88

Ha SH, Cho S (2008a) Level set based topological shape optimization of geometrically nonlinear structures using unstructured mesh. Comput Struct 86(13–14):1447–1455

Ha SH, Cho S (2008b) Level set-based topological shape optimization of nonlinear heat conduction problems. Numer Heat Transf, B Fundam 54(6):454–475

Haber E (2004) A multilevel, level-set method for optimizing eigenvalues in shape design problems. J Comput Phys 198(2):518–534

Haber RB, Bendsøe MP (1998) Problem formulation, solution procedures and geometric modeling–key issues in variable-topology optimization. In: 7th AIAA/USAF/NASA/ISSMO symposium on multidisciplinary analysis and optimization, St. Louis, MO, pp 1864–1873

Haber RB, Jog CS, Bendsøe MP (1996) A new approach to variable-topology shape design using a constraint on perimeter. Struct Optim 11(1):1–12

Hartmann D, Meinke M, Schröder W (2010) The constrained reinitialization equation for level set methods. J Comput Phys 229(5):1514–1535

Hassani B, Hinton E (1998) A review of homogenization and topology optimization. I–Homogenization theory for media with periodic structure. Comput Struct 69(6):707–717

He L, Kao CY, Osher S (2007) Incorporating topological derivatives into shape derivatives based level set methods. J Comput Phys 225(1):891–909

Hirsch C (2007) Numerical computation of internal and external flows: fundamentals of computational fluid dynamics, vol 1. Butterworth-Heinemann, Oxford

Ho HS, Lui BFY, Wang MY (2011) Parametric structural optimization with radial basis functions and partition of unity method. Optim Methods Softw 26(4–5):533–553

Ho HS, Wang MY, Zhou MD (2012) Parametric structural optimization with dynamic knot RBFs and partition of unity method. Struct Multidisc Optim 1–13. doi:10.1007/s00158-012-0848-7

Huang X, Xie M (2010) Evolutionary topology optimization of continuum structures: methods and applications. Wiley, New York

Iga A, Nishiwaki S, Izui K, Yoshimura M (2009) Topology optimization for thermal conductors considering design-dependent effects, including heat conduction and convection. Int J Heat Mass Transfer 52(11–12):2721–2732

Kao CY, Osher S, Yablonovitch E (2005) Maximizing band gaps in two-dimensional photonic crystals by using level set methods. Appl Phys, B Lasers Opt 81(2):235–244

Kawamoto A, Matsumori T, Yamasaki S, Nomura T, Kondoh T, Nishiwaki S (2011) Heaviside projection based topology optimization by a PDE-filtered scalar function. Struct Multidisc Optim 44(1):19–24

Khalil H, Bila S, Aubourg M, Baillargeat D, Verdeyme S, Jouve F, Delage C, Chartier T (2010) Shape optimized design of microwave dielectric resonators by level-set and topology gradient methods. Int J RF Microw Comput-Aided Eng 20(1):33–41

Kim MG, Ha SH, Cho S (2009) Level set-based topological shape optimization of nonlinear heat conduction problems using topological derivatives. Mech Des Struct Mach 37(4):550–582

Kreisselmeier G, Steinhauser R (1979) Systematic control design by optimizing a vector performance index. In: International federation of active controls symposium on computer-aided design of control systems, Zürich

Kreissl S, Maute K (2012) Level set based fluid topology optimization using the extended finite element method. Multidisc Optim 46(3):311–326

Kreissl S, Pingen G, Maute K (2011) An explicit level set approach for generalized shape optimization of fluids with the lattice Boltzmann method. Int J Numer Methods Fluids 65(5):496–519

Kwak J, Cho S (2005) Topological shape optimization of geometrically nonlinear structures using level set method. Comput Struct 83(27):2257–2268

Lazarov BS, Sigmund O (2011) Filters in topology optimization based on Helmholtz-type differential equations. Int J Numer Methods Eng 86(6):765–781

Le C, Bruns T, Tortorelli DA (2011) A gradient-based, parameter-free approach to shape optimization. Comput Methods Appl Mech Eng 200(9–12):985–996

Lim S, Yamada T, Min S, Nishiwaki S (2011) Topology optimization of a magnetic actuator based on a level set and phase-field approach. IEEE Trans Magn 47(5):1318–1321

Liu Z, Korvink JG (2008) Adaptive moving mesh level set method for structure topology optimization. Eng Optim 40(6):529–558

Liu Z, Korvink JG, Huang R (2005) Structure topology optimization: fully coupled level set method via FEMLAB. Struct Multidisc Optim 29(6):407–417

Luo Z, Tong L (2008) A level set method for shape and topology optimization of large-displacement compliant mechanisms. Int J Numer Methods Eng 76(6):862–892

Luo Z, Tong L, Wang MY, Wang S (2007) Shape and topology optimization of compliant mechanisms using a parameterization level set method. J Comput Phys 227(1):680–705

Luo J, Luo Z, Chen L, Tong L, Wang MY (2008a) A semi-implicit level set method for structural shape and topology optimization. J Comput Phys 227(11):5561–5581

Luo J, Luo Z, Chen S, Tong L, Wang MY (2008b) A new level set method for systematic design of hinge-free compliant mechanisms. Comput Methods Appl Mech Eng 198(2):318–331

Luo Z, Wang MY, Wang S, Wei P (2008c) A level set-based parameterization method for structural shape and topology optimization. Int J Numer Methods Eng 76(1):1–26

Luo Z, Tong L, Luo J, Wei P, Wang MY (2009a) Design of piezoelectric actuators using a multiphase level set method of piecewise constants. J Comput Phys 228(7):2643–2659

Luo Z, Tong L, Ma H (2009b) Shape and topology optimization for electrothermomechanical microactuators using level set methods. J Comput Phys 228(9):3173–3181

Luo Z, Zhang N, Gao W, Ma H (2012) Structural shape and topology optimization using a meshless Galerkin level set method. Int J Numer Methods Eng 90(3):369–389

Lyra PRM, Morgan K (2000a) A review and comparative study of upwind biased schemes for compressible flow computation. Part I: 1-D firstorder schemes. Arch Comput Methods Eng 7(1):19–55

Lyra PRM, Morgan K (2000b) A review and comparative study of upwind biased schemes for compressible flow computation. Part II: 1-D higher-order schemes. Arch Comput Methods Eng 7(3):333–377

Lyra PRM, Morgan K (2002) A review and comparative study of upwind biased schemes for compressible flow computation. Part III: Multidimensional extension on unstructured grids. Arch Comput Methods Eng 9(3):207–256

Malladi R, Sethian JA, Vemuri BC (1995a) Shape modeling with front propagation: a level set approach. IEEE Trans Pattern Anal Mach Intell 17(2):158–175

Malladi R, Sethian JA, Vemuri BC (1995b) Shape modeling with front propagation: a level set approach. IEEE Trans Pattern Anal Mach Intell 17(2):158–175

Marchuk GI (1990) Splitting and alternating direction methods. Handb Numer Anal 1:197–462
Maute K, Schwarz S, Ramm E (1998) Adaptive topology optimization of elastoplastic structures. Struct Multidisc Optim 15(2):81–91
Maute K, Kreissl S, Makhija D, Yang R (2011) Topology optimization of heat conduction in nano-composites. In: 9th World congress on structural and multidisciplinary optimization, Shizuoka, Japan
Mohamadian M, Shojaee S (2012) Binary level set method for structural topology optimization with MBO type of projection. Int J Numer Methods Eng 89(5):658–670
Myśliński A (2008) Level set method for optimization of contact problems. Eng Anal Bound Elem 32(11):986–994
Norato J, Haber R, Tortorelli DA, Bendsøe MP (2004) A geometry projection method for shape optimization. Int J Numer Methods Eng 60(14):2289–2312
Norato JA, Bendsøe MP, Haber RB, Tortorelli DA (2007) A topological derivative method for topology optimization. Struct Multidisc Optim 33(4):375–386
Novotny AA, Feijóo RA, Taroco E, Padra C (2003) Topological sensitivity analysis. Comput Methods Appl Mech Eng 192(7–8):803–829
Olsson E, Kreiss G, Zahedi S (2007) A conservative level set method for two phase flow II. J Comput Phys 225(1):785–807
Osher S, Fedkiw RP (2001) Level set methods: an overview and some recent results. J Comput Phys 169(2):463–502
Osher S, Fedkiw RP (2003) Level set methods and dynamic implicit surfaces, vol 153. Springer, New York
Osher S, Paragios N (2003) Geometric level set methods in imaging, vision, and graphics. Springer, New York
Osher SJ, Santosa F (2001) Level set methods for optimization problems involving geometry and constraints: I. Frequencies of a two-density inhomogeneous drum. J Comput Phys 171(1):272–288
Osher S, Sethian JA (1988) Fronts propagating with curvature-dependent speed: algorithms based on Hamilton–Jacobi formulations. J Comput Phys 79(1):12–49
Otomori M, Yamada T, Izui K, Nishiwaki S (2011) Level set-based topology optimisation of a compliant mechanism design using mathematical programming. Mech Sci 2(1):91–98
Park KS, Youn SK (2008) Topology optimization of shell structures using adaptive inner-front (AIF) level set method. Struct Multidisc Optim 36(1):43–58
Petersson J (1999) Some convergence results in perimeter-controlled topology optimization. Comput Methods Appl Mech Eng 171(1–2):123–140
Pingen G, Waidmann M, Evgrafov A, Maute K (2010) A parametric level-set approach for topology optimization of flow domains. Struct Multidisc Optim 41(1):117–131
Pironneau O (1989) Finite element method for fluids. Wiley, Chichester, England and New York/John Wiley and Sons, Paris
Rong JH, Liang QQ (2008) A level set method for topology optimization of continuum structures with bounded design domains. Comput Methods Appl Mech Eng 197(17–18):1447–1465
Rozvany GIN (2001) Aims, scope, methods, history and unified terminology of computer-aided topology optimization in structural mechanics. Struct Multidisc Optim 21(2):90–108
Rozvany GIN (2009) A critical review of established methods of structural topology optimization. Struct Multidisc Optim 37(3):217–237
Rozvany GIN, Zhou M (1991) The COC algorithm, part I: cross-section optimization or sizing. Comput Methods Appl Mech Eng 89(1–3):281–308
Rozvany GIN, Zhou M, Birker T (1992) Generalized shape optimization without homogenization. Struct Multidisc Optim 4(3):250–252
Rozvany GIN, Bendsøe MP, Kirsch U (1995) Layout optimization of structures. Appl Mech Rev 48:41
Schleupen A, Maute K, Ramm E (2000) Adaptive FE-procedures in shape optimization. Struct Multidisc Optim 19(4):282–302
Schumacher A (1995) Topologieoptimierung von bauteilstrukturen unter verwendung von lopchpositionierungkrieterien. PhD thesis, Universität-Gesamthochschule Siegen, Siegen, Germany
Sethian JA (1999) Level set methods and fast marching methods: evolving interfaces in computational geometry, fluid mechanics, computer vision, and materials science. Cambridge University Press, Cambridge
Sethian JA (2001) Evolution, implementation, and application of level set and fast marching methods for advancing fronts. J Comput Phys 169(2):503–555
Sethian JA, Smereka P (2003) Level set methods for fluid interfaces. Annu Rev Fluid Mech 35(1):341–372
Sethian JA, Wiegmann A (2000) Structural boundary design via level set and immersed interface methods. J Comput Phys 163(2):489–528
Shim H, Ho VTT, Wang S, Tortorelli DA (2008) Topological shape optimization of electromagnetic problems using level set method and radial basis function. Comput Model Eng Sci 37(2):175–202
Shojaee S, Mohammadian M (2011) A binary level set method for structural topology optimization. Int J Optim Civil Eng 1:73–90
Sigmund O (1994) Design of material structures using topology optimization. PhD thesis, Department of Solid Mechanics, Technical University of Denmark
Sigmund O (2007) Morphology-based black and white filters for topology optimization. Struct Multidisc Optim 33(4–5):401–424
Sigmund O (2011) On the usefulness of non-gradient approaches in topology optimization. Struct Multidisc Optim 43:589–596
Sigmund O, Maute K (2012) Sensitivity filtering from a continuum mechanics perspective. Struct Multidisc Optim 46(4):471–475
Sigmund O, Petersson J (1998) Numerical instabilities in topology optimization: a survey on procedures dealing with checkerboards, mesh-dependencies and local minima. Struct Multidisc Optim 16(1):68–75
Sokołowski J, Żochowski A (1999) On the topological derivative in shape optimization. SIAM J Control Optim 37(4):1251–1272
Sokołowski J, Żochowski A (2001) Topological derivatives of shape functionals for elasticity systems. Mech Struct Mach 29(3):331–349
Sokołowski J, Zolésio JP (1992) Introduction to shape optimization; shape sensitivity analysis. In: Springer series in computational mathematics, vol 16. Springer
Stolpe M, Svanberg K (2001) An alternative interpolation scheme for minimum compliance topology optimization. Struct Multidisc Optim 22(2):116–124
Strain J (1999) Semi-Lagrangian methods for level set equations. J Comput Phys 151(2):498–533
Sussman M, Smereka P, Osher S (1994) A level set approach for computing solutions to incompressible two-phase flow. J Comput Phys 114(1):146–159
Suzuki K, Kikuchi N (1991) A homogenization method for shape and topology optimization. Comput Methods Appl Mech Eng 93(3):291–318
Svanberg K (1987) The method of moving asymptotes—a new method for structural optimization. Int J Numer Methods Eng 24(2):359–373
Swan CC, Kosaka I (1997) Voigt–Reuss topology optimization for structures with nonlinear material behaviors. Int J Numer Methods Eng 40(20):3785–3814
Takezawa A, Nishiwaki S, Kitamura M (2010) Shape and topology optimization based on the phase field method and sensitivity analysis. J Comput Phys 229(7):2697–2718
Tikhonov AN, Goncharsky AV, Stepanov VV, Yagola AG (1995) Numerical methods for the solution of ill-posed problems. Springer, New York

Van Dijk NP, Yoon GH, Van Keulen F, Langelaar M (2010) A level-set-based topology optimization using the element connectivity parameterization method. Struct Multidisc Optim 42(2):269–282

Van Dijk NP, Langelaar M, Van Keulen F (2012) Explicit level-set-based topology optimization using an exact Heaviside function and consistent sensitivity analysis. Int J Numer Methods Eng 91(1):67–97

Van Keulen F, Haftka RT, Kim NH (2005) Review of options for structural design sensitivity analysis. Part 1: Linear systems. Comput Methods Appl Mech Eng 194(30–33):3213–3243

Van Miegroet L, Duysinx P (2007) Stress concentration minimization of 2D filets using X-FEM and level set description. Struct Multidisc Optim 33(4):425–438

Van Miegroet L, Moës N, Fleury C, Duysinx P (2005) Generalized shape optimization based on the level set method. In: 6th World congress of structural and multidisciplinary optimization

Wang MY, Wang X (2004a) "Color" level sets: a multi-phase method for structural topology optimization with multiple materials. Comput Methods Appl Mech Eng 193(6–8):469–496

Wang MY, Wang X (2004b) PDE-driven level sets, shape sensitivity and curvature flow for structural topology optimization. Comput Model Eng Sci 6:373–396

Wang MY, Wang X (2005) A level-set based variational method for design and optimization of heterogeneous objects. Comput-Aided Des 37(3):321–337

Wang S, Wang MY (2006a) A moving superimposed finite element method for structural topology optimization. Int J Numer Methods Eng 65(11):1892–1922

Wang S, Wang MY (2006b) Radial basis functions and level set method for structural topology optimization. Int J Numer Methods Eng 65(12):2060–2090

Wang MY, Zhou S (2004) Phase field: a variational method for structural topology optimization. Comput Model Eng Sci 6(6):547–566

Wang MY, Wang X, Guo D (2003) A level set method for structural topology optimization. Comput Methods Appl Mech Eng 192(1–2):227–246

Wang X, Wang MY, Guo D (2004) Structural shape and topology optimization in a level-set-based framework of region representation. Struct Multidisc Optim 27(1):1–19

Wang MY, Chen S, Wang X, Mei Y (2005) Design of multimaterial compliant mechanisms using level-set methods. J Mech Des 127:941–956

Wang SY, Lim KM, Khoo BC, Wang MY (2007a) An extended level set method for shape and topology optimization. J Comput Phys 221(1):395–421

Wang SY, Lim KM, Khoo BC, Wang MY (2007b) A geometric deformation constrained level set method for structural shape and topology optimization. Comput Model Eng Sci 18(3):155–181

Wang SY, Lim KM, Khoo BC, Wang MY (2007c) An unconditionally time-stable level set method and its application to shape and topology optimization. Comput Model Eng Sci 21(1):1–40

Wang F, Lazarov BS, Sigmund O (2011) On projection methods, convergence and robust formulations in topology optimization. Struct Multidisc Optim 43:767–784

Wei P, Wang MY (2006) Parametric structural shape and topology optimization method with radial basis functions and level-set method. In: Proceedings of international design engineering technical conferences & computers and information in engineering conference

Wei P, Wang MY (2009) Piecewise constant level set method for structural topology optimization. Int J Numer Methods Eng 78(4):379–402

Wei P, Wang MY, Xing X (2010) A study on X-FEM in continuum structural optimization using a level set model. Comput-Aided Des 42(8):708–719

Xia Q, Wang MY (2008) Topology optimization of thermoelastic structures using level set method. Comput Mech 42(6):837–857

Xie YM, Steven GP (1993) A simple evolutionary procedure for structural optimization. Comput Struct 49(5):885–896

Xing X, Wang MY, Lui BFY (2007) Parametric shape and topology optimization with moving knots radial basis functions and level set methods. In: 7th World congress on structural and multidisciplinary optimization, Seoul, Korea

Xing X, Wei P, Wang MY (2010) A finite element-based level set method for structural optimization. Int J Numer Methods Eng 82(7):805–842

Yamada T, Izui K, Nishiwaki S, Takezawa A (2010) A topology optimization method based on the level set method incorporating a fictitious interface energy. Comput Methods Appl Mech Eng 199(45–48):2876–2891

Yamada T, Izui K, Nishiwaki S (2011) A level set-based topology optimization method for maximizing thermal diffusivity in problems including design-dependent effects. J Mech Des 133:1–9

Yamasaki S, Nishiwaki S, Yamada T, Izui K, Yoshimura M (2010a) A structural optimization method based on the level set method using a new geometry-based re-initialization scheme. Int J Numer Methods Eng 83(12):1580–1624

Yamasaki S, Nomura T, Kawamoto A, Sato K, Izui K, Nishiwaki S (2010b) A level set based topology optimization method using the discretized signed distance function as the design variables. Struct Multidisc Optim 41(5):685–698

Yamasaki S, Nomura T, Kawamoto A, Sato K, Nishiwaki S (2011) A level set-based topology optimization method targeting metallic waveguide design problems. Int J Numer Methods Eng 87(9):844–868

Yanenko NN (1971) The method of fractional steps. Springer, Berlin

Yoon GH, Kim YY (2005) Element connectivity parameterization for topology optimization of geometrically nonlinear structures. Int J Solids Struct 42(7):1983–2009

Yulin M, Xiaoming W (2004a) A level set method for structural topology optimization and its applications. Adv Eng Softw 35(7):415–441

Yulin M, Xiaoming W (2004b) A level set method for structural topology optimization with multi-constraints and multi-materials. Acta Mech Sin 20(5):507–518

Zhou M, Rozvany GIN (1991) The COC algorithm, part II: topological, geometrical and generalized shape optimization. Comput Methods Appl Mech Eng 89(1–3):309–336

Zhou S, Li Q (2008) A variational level set method for the topology optimization of steady-state Navier–Stokes flow. J Comput Phys 227(24):10178–10195

Zhou JX, Zou W (2008) Meshless approximation combined with implicit topology description for optimization of continua. Struct Multidisc Optim 36(4):347–353

Zhou S, Wang MY (2007) Multimaterial structural topology optimization with a generalized Cahn–Hilliard model of multiphase transition. Struct Multidisc Optim 33(2):89–111

Zhou SW, Li W, Sun GY, Li Q (2010) A level-set procedure for the design of electromagnetic metamaterials. Opt Express 18(7):6693–6702

Zhu S, Liu C, Wu Q (2010) Binary level set methods for topology and shape optimization of a two-density inhomogeneous drum. Comput Methods Appl Mech Eng 199(45–48):2970–2986

Zhuang C, Xiong Z, Ding H (2009) Structural shape and topology optimization based on level-set modelling and the element-propagating method. Eng Optim 41(6):537–555

Zhuang CG, Xiong ZH, Ding H (2007) A level set method for topology optimization of heat conduction problem under multiple load cases. Comput Methods Appl Mech Eng 196(4–6):1074–1084

Zhuang C, Xiong Z, Ding H (2010) Topology optimization of multimaterial for the heat conduction problem based on the level set method. Eng Optim 42(9):811–831